Kastens, K. A., Mascle, J., et al., 1990
Proceedings of the Ocean Drilling Program, Scientific Results, Vol. 107

32. PLIOCENE-PLEISTOCENE CALCAREOUS NANNOFOSSIL DISTRIBUTION PATTERNS IN THE WESTERN MEDITERRANEAN[1]

D. Rio,[2] I. Raffi,[3] and G. Villa[3]

ABSTRACT

The distribution patterns of stratigraphically important calcareous nannofossils have been established in the Pliocene-Pleistocene of Site 653 sequence (Tyrrhenian Sea, Western Mediterranean). Semiquantitative and quantitative methods have been used to verify and improve biostratigraphic reliability of the nannofossil datums. Over twenty calcareous nannofossil events are considered reliable for biostratigraphic correlations based on the results of this study. Many of these events are not used in the existing zonal schemes, which rely, for the early Pliocene, upon events not easily detectable in the Mediterranean record. The need for a local zonal scheme is stressed for attaining a reproducible and highly resolved biostratigraphic classification. The zonal scheme we suggest provides an average time resolution of about 0.5 m.y. in the Pliocene and of about 0.2 m.y. in the Pleistocene.

INTRODUCTION

During Leg 107 of the Ocean Drilling Program (ODP), the *JOIDES Resolution* reoccupied the area of the rotary-drilled Deep Sea Drilling Project (DSDP) Site 132, located on a bathymetric terrace (Cornaglia Basin) in the Tyrrhenian Sea (Fig. 1). The sequence retrieved at DSDP Site 132 has been extensively studied (Cita, 1973; Raffi and Rio, 1979; Thunell, 1979) and is the most continuous Pliocene-Pleistocene deep-sea sequence available in the Western Mediterranean. The sequence represents a reference standard for the Italian mainland sections, which are the basis for Pliocene-Pleistocene stratigraphy.

Two holes (653A and 653B), located less than a kilometer from DSDP Site 132, were cored using the hydraulic piston corer (HPC) in order to recover a more complete record of this sequence for high-resolution biostratigraphic and paleoenvironmental studies.

In this chapter we report the results of a quantitative study of the distribution patterns of calcareous nannofossils in closely spaced samples from Holes 653A and 653B. Our aim is to address the problem of calcareous nannofossil biostratigraphic classification and resolution of the Pliocene-Pleistocene marine record of the Mediterranean region.

It is well known that during the Pliocene and Pleistocene the Mediterranean region acted as a distinct planktonic biogeographic province (Thunell, 1979; Berggren, 1984). Hence, regional biostratigraphic schemes have been developed for planktonic foraminifers by Cita (1973; 1975) and for calcareous nannofossils by Schmidt (1973), Müller (1978), Ellis (1979) and Raffi and Rio (1979). However, having been less affected by provincialism, calcareous nannofossils allow a fairly precise correlation between the Mediterranean regional schemes and the "standard" zonations of Martini (1971) and Okada and Bukry (1980) (Fig. 2). Therefore, they are the best suited fossil group for correlating the local Mediterranean with the extra-Mediterranean records.

Although the Mediterranean zonal schemes differ in terminology, stratigraphic resolution and boundary definitions, the ranking and spacing among most calcareous nannofossil events in the Mediterranean Pliocene-Pleistocene sequence is well established (Rio et al., 1984).

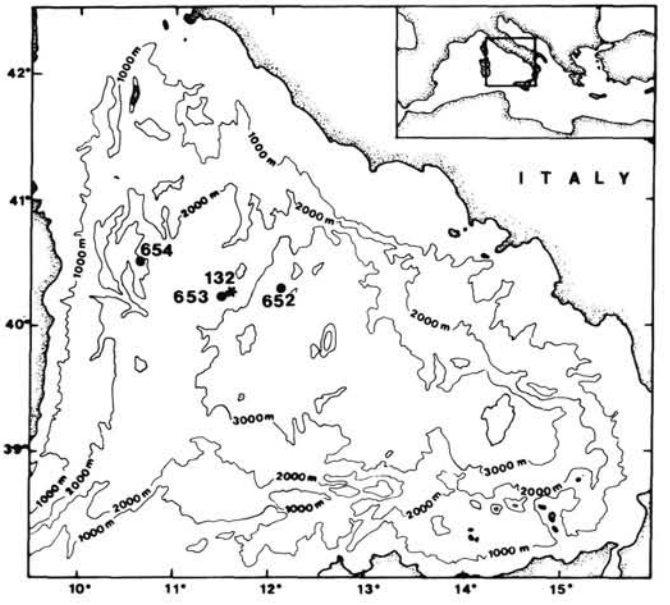

Figure 1. Location map showing positions of Sites 653 and 652, and DSDP Site 132.

Our goal is to test, as objectively as possible, the events used in Figure 2 and others reported in the most recent literature in the Site 653 sequence, in order to reconcile the various schemes and to improve stratigraphic resolution and reliability.

The results will serve as a stratigraphic framework for the paleoclimatic evolution of the Western Mediterranean, because magnetostratigraphic studies could not be carried out on this sequence (J. Channell, pers. comm., 1987).

STRATEGY

The calcareous nannofossil assemblages change through time because of evolutionary appearances (first appearance datums, or FADs) and extinctions (last appearance datums, or LADs) of taxa, and because environmental changes cause migrations (first occurrences, or FOs and last occurrences, or LOs) and fluctua-

[1] Kastens, K. A., Mascle, J., et al., 1990. *Proc. ODP, Sci. Results,* 107: College Station, TX (Ocean Drilling Program).

[2] Department of Geology and Paleontology, University of Padova, 35137 Padova, Italy.
[3] Department of Geology and Paleontology, University of Parma, 43100 Parma, Italy.

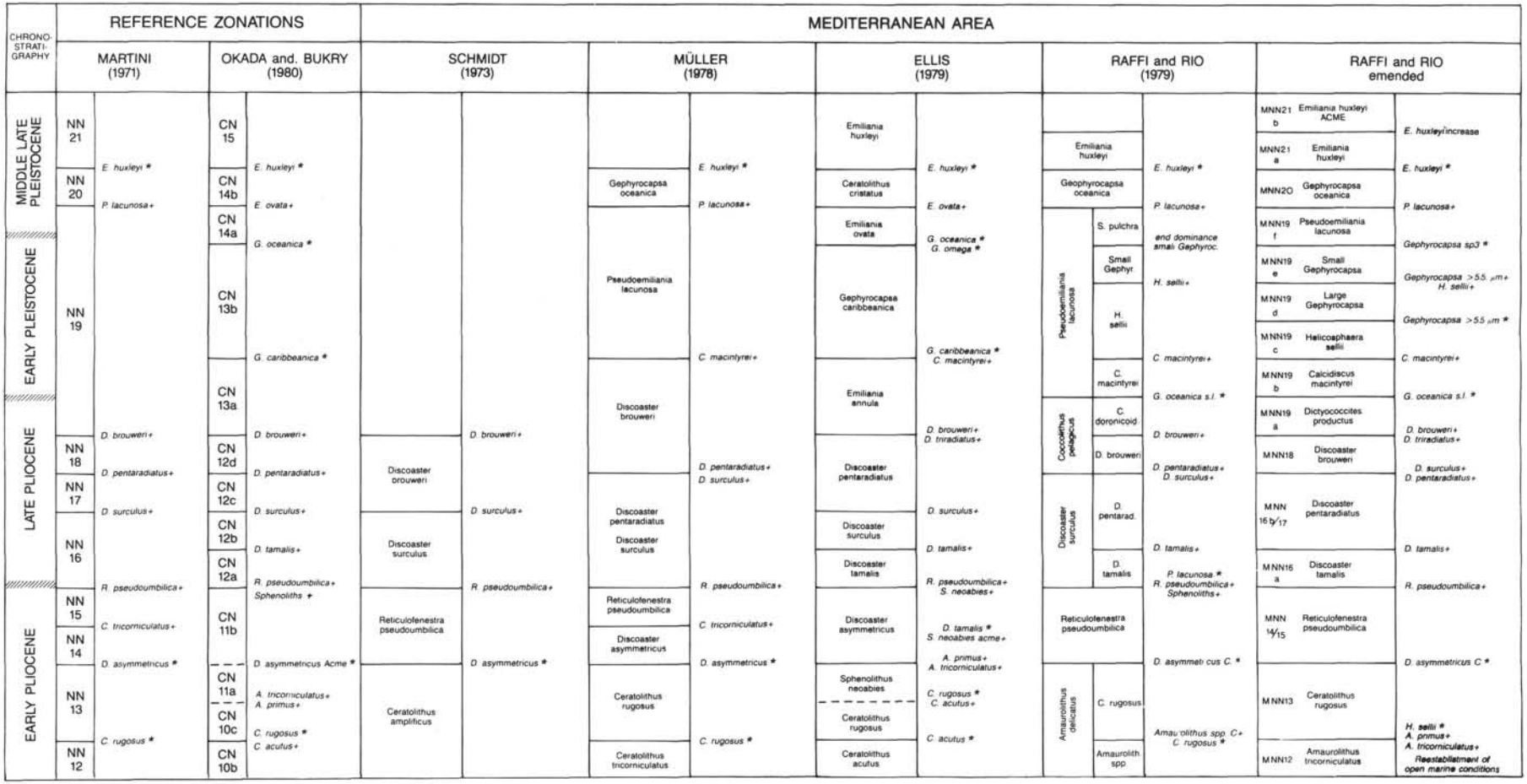

Figure 2. Calcareous nannofossil datum events and zonations proposed in the Mediterranean area compared with the "standard" zonations of Martini (1971) and Okada and Bukry (1980) for the Pliocene-Pleistocene interval. Key to symbols: + = extinction; * = appearance datum; MNN = Mediterranean Neogene Nannoplankton.

tions in presence and abundance of taxa (termed increase, acme, dominance, and absence) in different biogeographic provinces. Such floral changes, when distinct and correlatable, can serve as biostratigraphic events.

The Pliocene and Pleistocene were times of highly unstable climatic conditions and rapid evolutionary turnover in the calcareous nannoplankton. As a result, we have a large set of changes in the calcareous nannofossil assemblages which can be used for the purpose of biostratigraphic correlation. A list of the Pliocene-Pleistocene events, used for this purpose by different authors is reported in Table 1.

There have been recent discussions concerning the reliability of biostratigraphic events (Gradstein et al., 1985). Indeed, the most crucial aspect of a biostratigraphic event, which best qualifies its reliability, is its reproducibility in different sequences and among different authors. Reproducibility, and hence reliability of an event, is dependent upon the following factors:

1. the unambiguity of the taxonomic definition of the index species;
2. the distribution patterns of the index species, particularly its abundance and continuity and its mode of appearance and extinction;
3. distortions of the stratigraphic record due to reworking, sediment mixing, and taphonomic exclusion;
4. operational procedures such as sample collection (i.e., drilling disturbance, field, and laboratory contamination) and different methods of data collection and event definition;
5. ecologic and biogeographic requirements of the index species which control its distribution and, therefore, the traceability and synchroneity of the event.

In order to test and to improve the reliability of biostratigraphic events we have tried to minimize the above problems by adopting the following strategy:

1. We use biometric definitions whenever possible for taxa affected by taxonomic problems. Biometry can sometimes be cumbersome and impractical, but in our specific case we will show that plane size measurements can provide a basis for unequivocal biostratigraphic events; whenever events are defined by taxonomically difficult species (like *Pseudoemiliania lacunosa* FAD), they are scored as second order events.
2. We produce quantitative and semiquantitative data on the distribution patterns of the taxa listed in Table 1 in order to evaluate abundance, continuity, and modes of appearance and extinction of these index species. Backman and Shackleton (1983) have shown that quantitative or semiquantitative data allows estimation of the noise level in the stratigraphic record that results from reworking or operational procedures (i.e., downhole contamination, caving, etc.).
3. We provide an operational and quantitative definition of individual biostratigraphic events. Such definitions have seldom been used in nannofossil biostratigraphy. Indeed when applied, for example, to the LAD of *P. lacunosa* and the FAD of *E. huxleyi* (Thierstein et al., 1977), they prove to be extremely useful. For this operational definition the above-mentioned distribution features are essential. In proposing event definitions our concern was to develop methods which can be consistently applied by other biostratigraphers in different geologic settings.

A special comment is in order concerning the traceability and synchroneity of biostratigraphic events. Traceability of calcareous nannofossil events is generally very good because they can be recognized in different facies of the Mediterranean region (Rio et al., 1984; Rio et al., in press; Glaçon et al., this volume). Synchroneity, when verified, transforms a biostratigraphic event into a tool of biochronological age evaluation (Berggren and Van Couvering, 1978). The most objective way of evaluating synchroneity of a biostratigraphic event is through calibration with magnetostratigraphy (Berggren et al., 1985) or stable isotope stratigraphy (Thierstein et al., 1977). At Site 653 we can verify synchroneity of calcareous nannofossil events by means of oxygen isotope stratigraphy. Unfortunately it is not possible to calibrate the bioevents to magnetic stratigraphy. A test of the synchroneity of events not directly calibrated to the oxygen isotope record has been carried out by utilizing a modified "Shaw diagram" technique (see Appendix).

Table 1. List of calcareous nannofossils which have been used for biostratigraphic correlations and classification in the Pliocene-Pleistocene (listed top to bottom from oldest to youngest).

Triquetrorhabdulus rugosus LAD
Ceratolithus acutus FAD
Ceratolithus rugosus FAD
Amaurolithus primus LAD
Amaurolithus tricorniculatus LAD
Helicosphaera sellii FO
Discoaster asymmetricus FCO
Discoaster tamalis FAD
Sphenolithus neoabies Acme end
Amaurolithus delicatus LAD
Pseudoemiliania lacunosa FAD
Discoaster pentaradiatus (beginning paracme sensu Driever)
Reticulofenestra pseudoumbilica LAD
Sphenolithus spp. LAD
Discoaster pentaradiatus (end paracme sensu Driever)
Discoaster tamalis LAD
Discoaster surculus LAD
Discoaster pentaradiatus LAD
Discoaster triradiatus increase
Discoaster brouweri LAD
Gephyrocapsa oceanica s.l. FAD
Calcidiscus macintyrei LAD
Gephyrocapsa spp. >5.5 μm FAD
Helicosphaera sellii LAD
Gephyrocapsa spp. >5.5 μm LAD
small *Gephyrocapsa* spp. (beginning dominance)
small *Gephyrocapsa* spp. (end dominance)
Gephyrocapsa sp. 3 FAD
Pseudoemiliania lacunosa LAD
Emiliania huxleyi FAD
Emiliania huxleyi increase

METHODS

The distribution of the taxa listed in Table 1 (except for *Emiliania huxleyi*) were determined by light microscope technique (normal light and crossed nicols). Preparation of smear slides for light microscope examinations followed standard procedures. A small amount (5–10 mm^3) is smeared onto a glass slide, using a drop of water and a flat toothpick.

Data were collected by quantitative and semiquantitative methods. The application of quantitative methods to calcareous nannofossil biostratigraphy has been discussed at length by Backman and Shackleton (1983) and we have largely implemented their approach in our work.

The frequency of a species in a fossil assemblage depends on a complex interplay among species productivity, terrigenous or other microfossil dilution and dissolution. These factors have different effects on detecting the stratigraphic distribution of index species in different facies and they must be considered in selecting reproducible counting methods. Also important is a reasonable balance between time involved in counting and the resultant benefits.

In this work we have applied and tested three different counting methods: (1) index species vs. the total assemblage; (2) index species vs. a fixed number of taxonomically related forms; (3) number of specimens of the index species in a prefixed area of a slide. These are detailed in the following sections.

Counting the Index Species vs. the Total Assemblage

This is the most objective method and it has been applied by Thierstein et al. (1977) to the *P. lacunosa* LAD and the *E. huxleyi* FAD. It allows the confidence level of detecting a species to be specified depending on its frequency in the original population and on the sample size (Dennison and Hay, 1967). Normally, we have restricted counts to 500 specimens, which results in a probability of greater than 99% that a taxon will be encountered, if its true relative abundance in the population is <1% (Crow et al., 1960). This method is independent of terrigenous or other microfossil dilution, and it is relatively easy to perform in most samples. On the other hand, it presents the drawback that rare, but perhaps biostratigraphically important taxa (i.e., ceratolithids and discoasterids in the Mediterranean) will not be detected. Furthermore, when samples are affected by dissolution, the frequency data can be strongly biased by increasing the relative abundance of resistant species.

Counting the Index Species vs. a Fixed Number of Taxonomically Related Forms

This method was introduced by Backman and Shackleton (1983) for monitoring the *H. sellii* LAD, which was evaluated relative to a predetermined number of helicolithids, and for the *A. delicatus* LAD, which was evaluated relative to a predetermined number of ceratolithids. This method can only be applied when the reference group is well represented. By assuming that the reference group had similar preservational and ecological prerequisites, we can consider this method to be independent of preservation state, dilution, and paleoecological exclusion. Furthermore, the total number of specimens considered allows for the detection of events in both common and relatively rare species.

In the present work we have applied this method extensively because of these advantages (i.e., increase of sample size examined and independence of facies).

Counting the Number of Specimens of an Index Species in a Pre-fixed Area of the Slide

This method was applied by Raffi and Rio (1981) for evaluating the abundance patterns of ecologically significant taxa (*C. pelagicus, B. bigelowii,* etc.) and extensively used by Backman and coworkers in establishing the biochronology of Pliocene and Pleistocene calcareous nannofossil datum planes. It involves the counting of all specimens of a selected taxonomic unit in a predetermined number of fields of view at a specified magnification. The abundance data are expressed relative to the unit area of slide examined (number of specimens per square millimeter).

This method, which is very convenient, is better viewed as semiquantitative, but Backman and Shackleton (1983) have shown that it can provide surprisingly accurate data. However, it is clear that this method is influenced by the preparation technique (density of the material on the glass slide), and by dissolution and terrigenous dilution.

In the case of a pelagic sequence yielding virtually undissolved assemblages, as is the case for Site 653, this method provides the best combination of accuracy and rapidity for data collecting. Counts obtained by this method have been shown by Backman (1986) to be roughly proportional to the productivity of the species of interest, in cases where dissolution had negligible influence on accumulation. We will often refer to the counts produced by this method as "productivity curves." We have applied this method to most index species and, when cross-checked, it shows to provide data comparable with those collected with the previous two methods. However, it is unsuitable for comparing data from pelagic and terrigenous sequences and our operational definitions thus are based on the first and second methods.

Material

A total of 355 samples were examined for the present study, of which 350 are from Core 107-653A-1H through Core 107-653A-23X, with 5 samples from Core 107-653B-23X. The correlation between Holes 653A and 653B is based on the end of the *Sphaeroidinellopsis* spp. acme (R. Sprovieri, pers. comm., 1987).

A maximum sample spacing of 70 cm was used for those intervals where no biostratigraphic events occurred. This sample spacing represents roughly 25–30 k.y. based on the accumulation curve presented in Figure 11. However, for most of the sequence, and particularly at critical intervals (i.e., close to biostratigraphic events, across chronostratigraphic boundaries and climatic thresholds) the sample spacing was from 40 to 10 cm, representing a time interval shorter than 10 k.y.

RESULTS

The results obtained by the different counting methods outlined above are illustrated in Figures 3, 4, 5, 7, and 9. In the following sections we discuss the events listed in Table 1 in the light of the patterns presented in these Figures. The stratigraphic positions of these events are reported in Table 2.

Discoasters

Discoasterids are important constituents of the Pliocene calcareous nannofossil assemblages, and the succession of discoaster events (mainly LADs) was established at the very beginning of calcareous nannofossil biostratigraphy (Gartner, 1969; Bukry, 1973). Recently, Backman and Shackleton (1983), and Backman and Pestiaux (1987) have established a precise chronology of Pliocene discoaster evolution.

Graphs for the following *Discoaster* species have been plotted: *D. brouweri, D. triradiatus, D. pentaradiatus, D. surculus, D. intercalaris, D. asymmetricus, D. tamalis,* and *D. variabilis.*

These species do not present any taxonomic problems and we have followed the species concepts of Backman and Shackleton (1983). Most specimens included in *Discoaster* spp. have not been classified for preservational reasons and some of them represent undescribed endemic Mediterranean species.

The usefulness of discoasters in the Mediterranean has been questioned because of their alleged low abundance, especially late in their Western Mediterranean range.

We have plotted, for all discoaster categories listed above, both a "productivity curve" (Fig. 3) based on scanning an area of 4.15 mm^2, and the percentages of the single *Discoaster* species within a total count of 100 discoasters (Fig. 4).

The "productivity curves" represent the better picture of the stratigraphic distribution patterns of the species of interest. Although fundamental for locating the true appearance and extinction levels of species, we have defined *Discoaster* events on the basis of abundance in order to achieve a better reproducibil-

Table 2. Summary of the position of calcareous nannofossil events at Site 653.

Event	Core, section, interval (cm)		Depth (mbsf)
E. huxleyi increase	1H-3, 25	2H-1, 60	3.70 + 0.50
E. huxleyi FAD	3H-2, 60	3H-2, 120	15.60 + 0.30
P. lacunosa LAD	4H-5, 25	4H-5, 60	29.12 + 0.17
Gephyrocapsa sp. 3 FAD	7H-6, 25	7H-6, 59	58.92 + 0.17
Top small *Gephyrocapsa*	7H-6, 25	7H-6, 59	58.92 + 0.17
Gephyrocapsa spp. >5.5 μm LAD	8H-3, 120	8H-4, 25	64.97 + 0.27
H. sellii LAD	8H-4, 25	8H-4, 58	65.42 + 0.17
Gephyrocapsa spp. >5.5 μm FAD	9H-3, 60	9H-3, 100	73.80 + 0.20
C. macintyrei LAD	10H-1, 60	10H-1, 75	80.27 + 0.08
G. oceanica s.l. FAD	10H-4, 120	10H-5, 25	85.50 + 0.27
D. brouweri LAD	11H-1, 25	10H-6, 100	88.70 + 0.60
D. pentaradiatus LO	13H-2, 120	13H-3, 15	110.60 + 0.20
Discoaster decrease/ *D. surculus* LAD	13H-3, 58	13H-3, 100	111.49 + 0.20
D. asymmetricus LAD	14H-1, 60	14H-1, 100	118.10 + 0.20
D. tamalis LAD	14H-2, 25	14H-2, 60	119.22 + 0.17
D. pentaradiatus end paracme	17H-1, 60	17H-1, 100	146.40 + 0.20
Sphenolithus spp. LAD	17H-5, 25	17H-5, 60	152.00 + 0.17
R. pseudoumbilica LAD	18H-1, 120	18H-2, 25	156.60 + 0.27
D. pentaradiatus beginning paracme	18H-2, 100	18H-3, 24	158.00 + 0.37
P. lacunosa FAD	19H-1, 120	19H-2, 25	165.60 + 0.27
A. delicatus LAD	19H-2, 25	19H-2, 60	166.02 + 0.17
D. tamalis FAD	19H-3, 25	19H-3, 63	167.50 + 0.17
D. asymmetricus FCO	19H-4, 100	19H-5, 25	169.90 + 0.37
Amaurolithus spp. LCO	21H-2, 120	21H-3, 25	186.17 + 0.13
H. sellii FAD	21H-3, 120	21H-4, 25	187.67 + 0.27

ity in the terrigenous Italian mainland sections. However, the selected definitions are virtually the same for each of the two approaches.

The "productivity curves" indicate that this group is consistently present in the Mediterranean Pliocene record, although its abundance is much lower than in low-latitude sediments. This statement is supported by the comparison with Backman and Shackleton's curves (1983). While these authors counted as many as 500–700 discoasters per mm^2 in their slides of low-latitude sediments, we counted a maximum of 100 discoasters per mm^2 (Fig. 3). However, as expected, the productivity of discoasters in the Western Mediterranean was higher than in the northern North Atlantic DSDP Site 552 (compare our data in Fig. 3 with data in fig. 1 of Backman et al., 1986).

The total accumulation of *Discoaster* species (Fig. 3) shows short-term fluctuations within the frame of long-term fluctuations. Similar fluctuations were observed in the subtropical and northern Atlantic by Backman and Pestiaux (1987) and attributed to changes in the Earth's orbital parameters. The Western Mediterranean record shows some differences from the pattern evidenced in the subtropical Atlantic, where short-term fluctuations are overprinted on a general trend of decreasing abundances with decreasing ages. In contrast, in the Mediterranean the total abundance of discoasters increases in the mid-Pliocene.

A common feature of the Mediterranean, subtropical, and northern North Atlantic discoaster "productivity" records is the sharp decrease in abundance in the late Pliocene. Backman and Pestiaux (1987) associated this event with the onset of major Northern Hemisphere glaciation.

It is significant that at Site 653 the drop in discoasters corresponds with a permanent enrichment of $\delta^{18}O$ in planktonic foraminifers (Vergnaud-Grazzini et al., this volume).

After the sharp decline in abundance at about 2.4 Ma, discoasters (represented by *D. brouweri* and *D. triradiatus*) are absent during long intervals. A similar pattern has been observed by Backman and Pestiaux (1987) in the northern North Atlantic DSDP Site 552. It is tempting to correlate the presence of intervals of *D. brouweri* to migration events during times of climatically favorable conditions.

Comments on individual discoaster biostratigraphic events follow.

Discoaster asymmetricus and *Discoaster tamalis*

D. asymmetricus and *D. tamalis* are common elements of discoasterids in the Mediterranean Pliocene (Figs. 3 and 4). Their distribution provides two widely used bioevents: the first common occurrence (FCO) of *D. asymmetricus,* and the exit of *D. tamalis*. Both events are used in many biostratigraphic schemes (Fig. 2).

D. tamalis and *D. asymmetricus* are rare in the late Miocene (Raffi and Rio, 1979). In the present work *D. tamalis* is not recorded in the early early Pliocene; *D. asymmetricus* is rare and occurs in few samples, up to the latest part of the early Pliocene, at which point it is common and continuously present (Figs. 3 and 4). Its first common and continuous occurrence (FCO) is, therefore, an event that can be used for correlation and classification. We define this event as the point at which *D. asymmetricus* reaches a >5% frequency in a count of 100 discoasters.

This event has been directly calibrated to the magnetic reversal time scale in Mediterranean Sites 652 and 654, where it occurs just above the Cochiti subchron at an age of about 3.81–3.85 Ma (Channell et al., this volume).

D. tamalis enters the stratigraphic record slightly above the *D. asymmetricus* FCO, at a high level of abundance. In spite of short absence intervals in the lower parts of its range (Figs. 3 and 4), it provides an easily detected event in the late early Pliocene. The *D. tamalis* FO is not used in the existing biostratigraphic schemes, but it is nonetheless useful in biostratigraphic analysis.

Backman and Shackleton (1983), Backman and Pestiaux (1987), and Backman et al. (1986) demonstrated that *D. tamalis* and *D. asymmetricus* exhibit pronounced covariation in abundance patterns during most of their ranges in the equatorial Pacific (Core V28-179), the North Pacific (Core V32-127), the northern North Atlantic (DSDP Hole 552A) and the subtropical North Atlantic (DSDP Site 606). A fair degree of covariation is also seen in the Western Mediterranean record (Figs. 3 and 4), reinforcing Backman and Pestiaux's (1987) suggestion that this pattern of covariation occurred on a global scale and that a close taxonomic relationship probably existed between *D. tamalis* and *D. asymmetricus*.

Also noteworthy is the good inverse correlation between *D. tamalis/D. asymmetricus* and *D. pentaradiatus* (Figs. 3 and 4), which suggests different ecologic preferences. Considering Bukry's (1981) paleobiogeographic data, it is easy to infer a warm-water preference to *D. pentaradiatus* and a cooler-water preference to *D. tamalis/D. asymmetricus*.

D. asymmetricus and *D. tamalis* become extinct simultaneously in our sequence, although in the upper parts of their ranges they are not abundant, being subordinate to *D. pentaradiatus* in the discoaster population.

We consider the exit of *D. tamalis* to be a good biostratigraphic event in the Mediterranean, and is defined as the decrease of the species to less than 2% in our 100-discoaster counts. A close sampling interval is necessary to properly detect this event because, in some samples just below the extinction, *D. tamalis* is absent or very rare (Figs. 3 and 4).

Discoaster surculus and *Discoaster pentaradiatus*

D. surculus and *D. pentaradiatus* appeared in the late Miocene and became extinct in the late Pliocene. Both the *D. surculus* LAD and the *D. pentaradiatus* LAD are used in many biostratigraphic schemes (Fig. 2), although their mutual relationship is debated. In many oceanic areas *D. surculus* disappears slightly earlier than *D. pentaradiatus,* allowing the definition of the NN17 Zone of Martini (1971) and of the CNl2c subzone of Okada and Bukry (1980). In the Mediterranean the two events have been detected very close to each other, making the recognition of the above biostratigraphic interval impossible (Müller, 1978; Ellis, 1979; Raffi and Rio, 1979).

At Site 653, *D. surculus* ceases to be continuously present at 11.40 mbsf in coincidence with the drop in abundance of other discoasters. In the next overlying sample (110.60 mbsf), which contains very few discoasterids, *D. pentaradiatus* is still present in high percentage relative to other discoasters. Immediately above this level discoasterids are very rare. It is virtually impossible to decide if the few specimens of *D. surculus* and *D. pentaradiatus* recorded in this interval are indigenous or reworked.

For practical purposes of performing stratigraphic correlations, the exits of *D. surculus* and *D. pentaradiatus* can be considered simultaneous in the Mediterranean and coincident with a significant drop in the discoaster abundance. These features provide a biostratigraphic signal which is easily correlatable and which coincides with an enrichment in $\delta^{18}O$ in planktonic foraminifers (Vergnaud Grazzini et al., this volume), thus suggesting a correlation with the onset of the Northern Hemisphere Glaciation (Shackleton et al., 1984).

In the northern North Atlantic DSDP Hole 552A, Backman and Pestiaux (1987) found the exit of *D. surculus* in conjunction with the first pulse of ice-rafted material at about 2.4 Ma, and the exit of *D. pentaradiatus* in conjunction with a second cycle of ice-rafting. We can speculate that this climatic event might

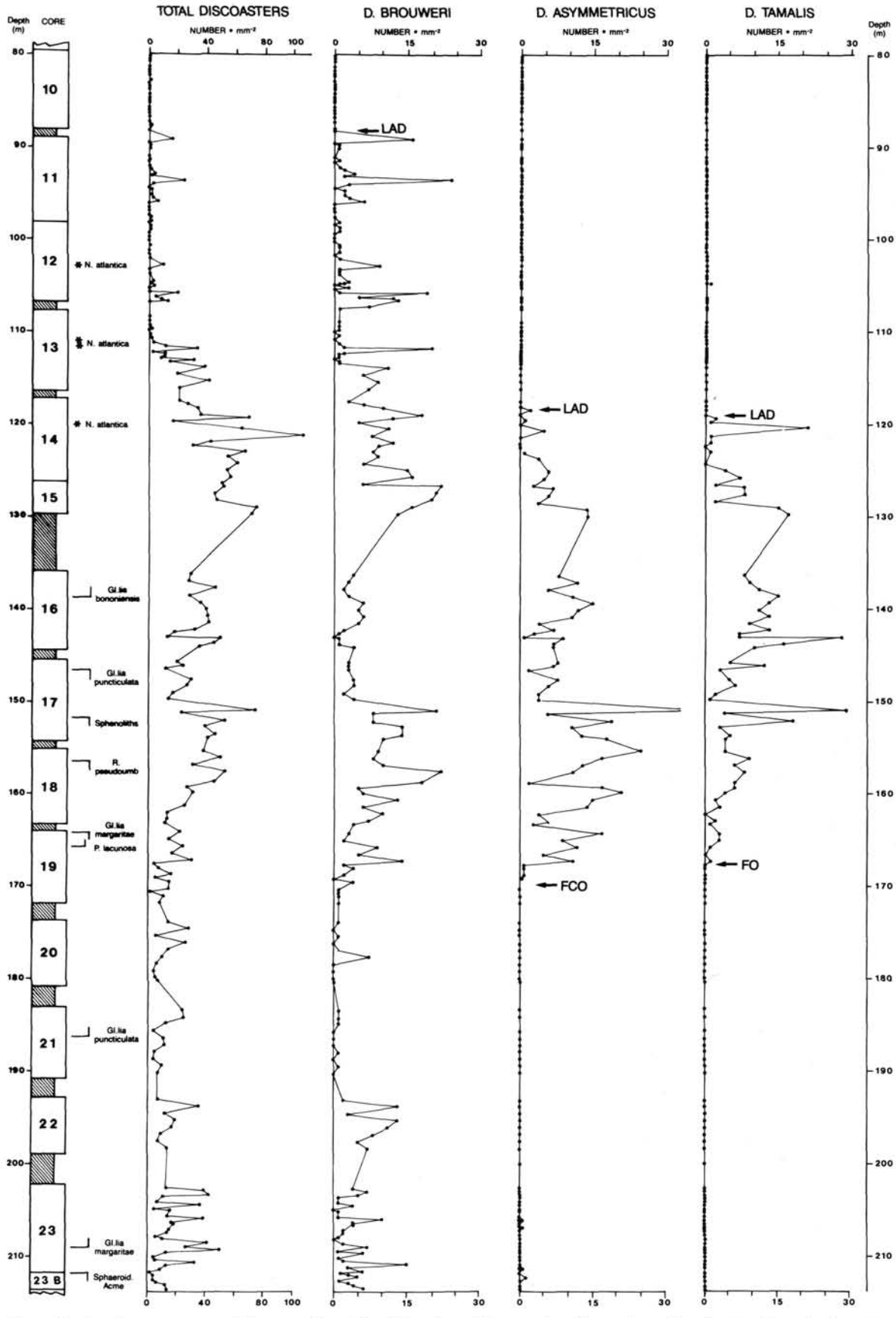

Figure 3. Abundance patterns of discoasterids at Site 653 evaluated by counting the number of specimens of species in a prefixed area of a slide. Planktonic foraminiferal data are from Glaçon et al. (this volume). Key to symbols: ⌊ = appearance; ⌉ = extinction; * = presence.

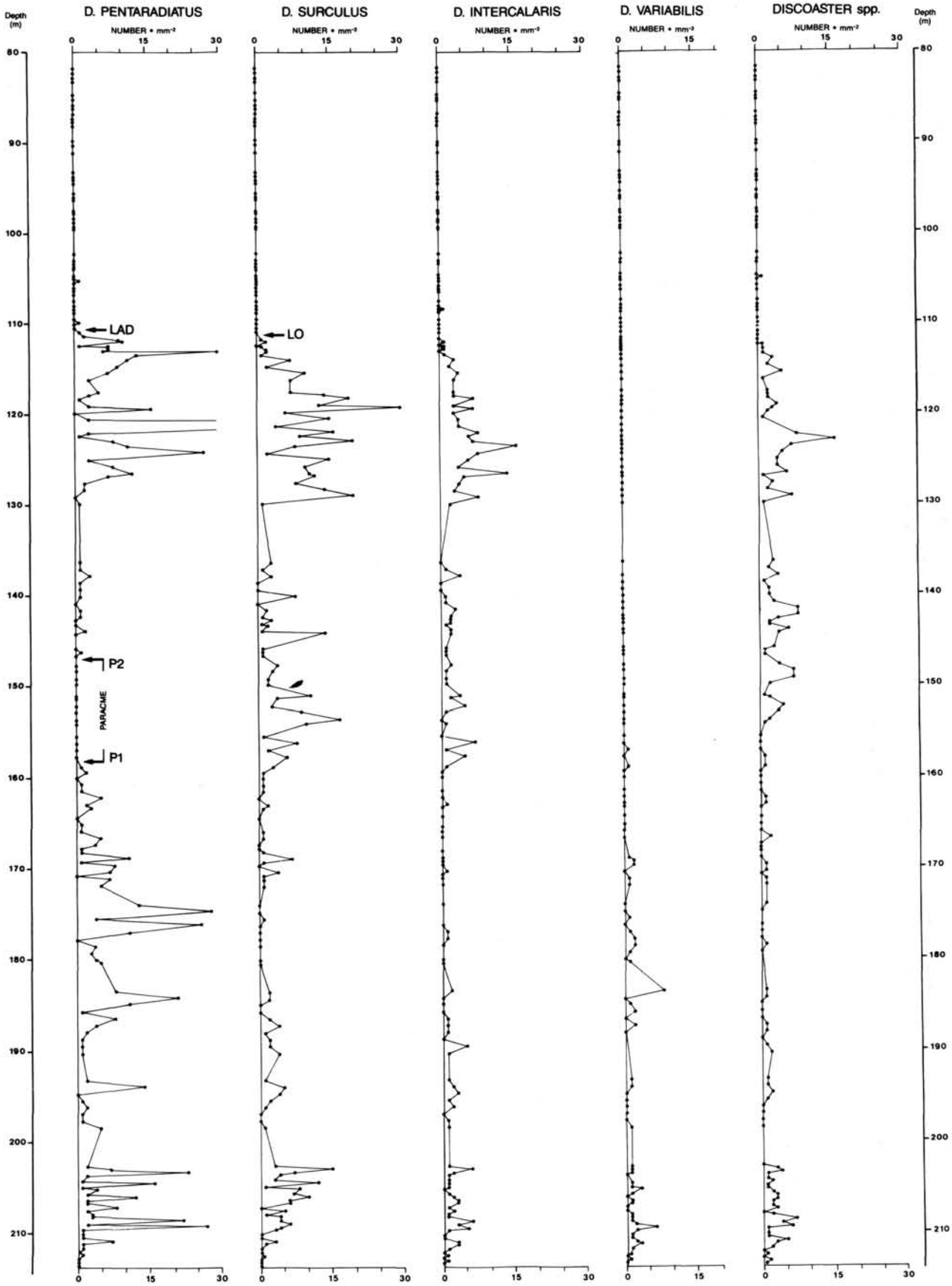

Figure 3 (continued).

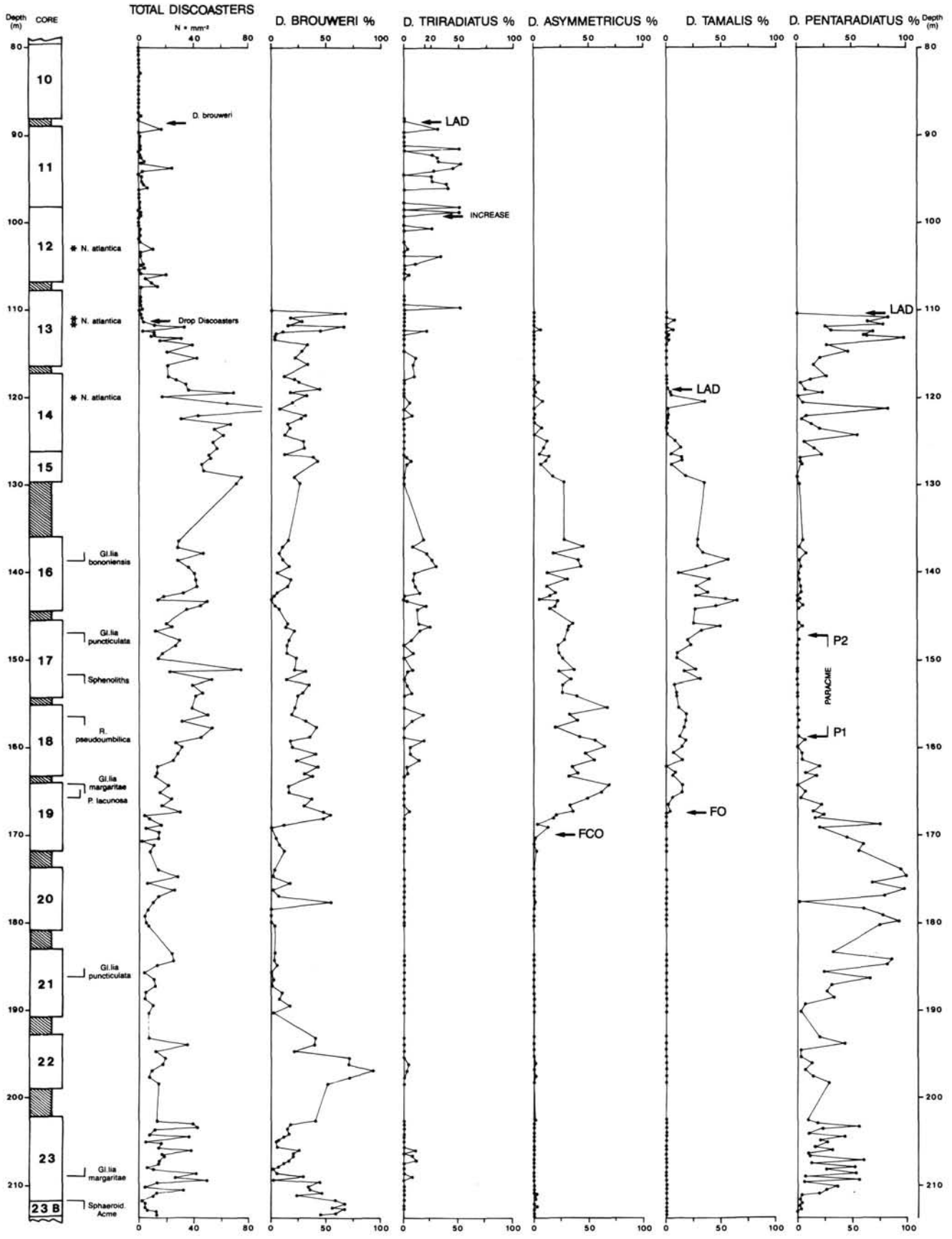

Figure 4. Abundance of discoasterids relative to 100 specimens of *Discoaster* spp. Note that percentages of *D. triradiatus* are plotted vs. the total number of *D. brouweri* (see discussion in the text). For reference, the curve of the total abundance of discoasters encountered in a prefixed area of a slide and other calcareous plankton biostratigraphic events are reported.

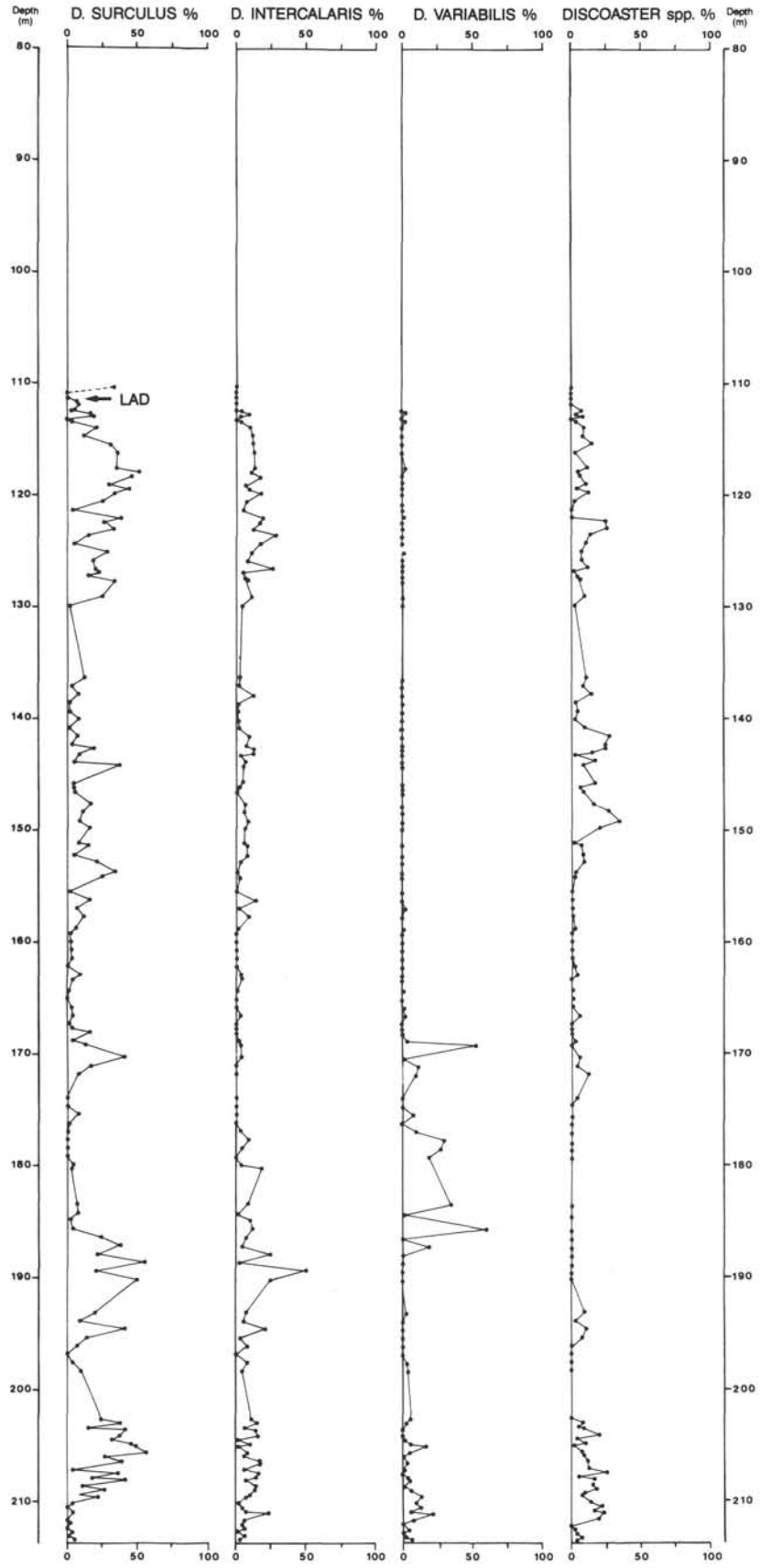

Figure 4 (continued).

have excluded the upper part of *D. pentaradiatus*'s range from the Mediterranean record.

Discoaster pentaradiatus Paracme

Driever (1981) noted that *D. pentaradiatus* shows a peculiar distribution in the Mediterranean, being virtually absent at the transition between the early and late Pliocene. On the basis of this feature, he defined a "*D. pentaradiatus* paracme Zone" which is nicely detected in our plots (Figs. 3 and 4). Although, we do not use the beginning and the end of the *D. pentaradiatus* paracme in our zonation, we consider both these events as useful for very fine biostratigraphic subdivision, as they were observed in all the Mediterranean sections thus far investigated in detail (Driever, 1981; Rio et al., in preparation).

Discoaster brouweri and *Discoaster triradiatus*

D. brouweri is the last representative of the discoasterids in the late Pliocene, and its extinction (Ericson et al., 1963) is used in all the low- and middle-latitude zonations. Its utility in the Western Mediterranean and in the high-latitude areas has been questioned by some authors (i.e., Müller, 1978). Our plot indicates that *D. brouweri* is actually discontinuously present, at low levels of abundance, in the late Pliocene. In the intervals where it is present, up to 20–30 specimens occur per mm^2. This is a much greater abundance than *Ceratolithus rugosus* and *Amaurolithus delicatus* in the early Pliocene. Its discontinuous presence is easily detected, provided that the sampling intervals are close and the terrigenous dilution is not overwhelming.

The last occurrence of *D. brouweri* has been directly calibrated in the Mediterranean to the magnetic reversal time scale in southern Italy (Backman et al, 1983) and at Site 652 (Channell et al., this volume) as occurring very close to the base of the Olduvai subchron, at an estimated age which approximates that found low latitudes (Fig. 11 and Table 3). We see no reason to exclude it from the biostratigraphic classification of the Western Mediterranean, although it represents a more difficult datum to detect in the stratigraphic sequence.

It has been long known that the three-rayed variety of *D. brouweri* (*D. triradiatus*) became particularly abundant late in the species' range (Takayama, 1970). Backman and Shackleton (1983) introduced a datum defined by the increase in the proportion (>20%) of *D. triradiatus* relative to *D. brouweri.* The age of this event at DSDP Site 606 (North Atlantic) was estimated by Backman and Pestiaux (1987) to be 2.07 Ma.

We have produced a plot of the percentages of *D. triradiatus* vs. *D. brouweri* throughout the Pliocene (Fig. 4). It can be seen that this form is more common in the Mediterranean than at DSDP Site 606, and the event is not as distinct as in extra-Mediterranean areas. Nevertheless, continuous high abundance is typical of the latest parts of *D. brouweri*'s range. We tentatively use the increase above 40% of *D. triradiatus* relative to *D. brouweri* as a biostratigraphic event in the Mediterranean. This is the only definition which is unequivocal in the Western Mediterranean record. The interpolated age of the *D. triradiatus* increase derived in the Appendix compares well with that estimated by Backman and Pestiaux (1987) in the Northern Atlantic (Table 3).

The *D. triradiatus* increase is herein considered a secondary event in the Mediterranean, but it can be useful for subdividing the long interval between the drop in abundance of discoasterids and the *D. brouweri* final exit.

At Site 653 *D. triradiatus* becomes extinct with *D. brouweri,* as it does in extra-Mediterranean sequences (Backman and Shackleton, 1983).

Discoaster variabilis

D. variabilis is not used in the biostratigraphic classification of the Pliocene. In the low-latitude oceanic sediments it becomes extinct in the late Pliocene (Bukry, 1973). At Site 653 it shows a peculiar distribution, being virtually restricted to the early Pliocene (Figs. 3 and 4). It becomes particularly abundant with the entrance of *G. puncticulata* and becomes practically absent with the entrances of *D. tamalis* and *D. asymmetricus,* in an interval of strong turnover in the calcareous nannofossil assemblage.

Early Pliocene Coccolith Datum Events

In this section we discuss the early Pliocene datums based on all calcareous nannofossils, other than discoasterids, listed in Table 1. Quantitative distribution patterns of these nannofossils are illustrated in Figure 5.

Triquetrorhabdulus rugosus

Triquetrorhabdulus rugosus extinction has been used by Okada and Bukry (1980) as a secondary event to recognize the CN10a/CN10b subzonal boundary, which is defined primarily by the *C. acutus* FAD. *T. rugosus* has not been found at Site 653, but it has been reported in the Mediterranean basal Pliocene (MPl 1) at Capo Rossello section (Rio et al., 1984) and at Capo Spartivento section, Calabria, and Site 652 (I. Raffi, unpubl. data).

Ceratoliths

The ceratholithid group provides the main events used in the standard zonations for subdividing the latest Miocene and the early Pliocene: *Ceratolithus acutus* FAD, *C. rugosus* FAD and *Amaurolithus delicatus* LAD.

The group is poorly represented in the Western Mediterranean (Fig. 5). In the early early Pliocene *Amaurolithus* spp. (represented by the three species *A. delicatus, A. primus,* and *A. tricorniculatus*) are fairly continuous, albeit in low abundance (maximum value = 3 *Amaurolithus* spp. per mm^2; see Fig. 5). Above this level, *A. tricorniculatus* and *A. primus* disappear and *A. delicatus* is detected in discrete intervals at very low levels of abundance (maximum value = 0.5 specimens per mm^2).

Raffi and Rio (1979) subdivided the NN12–NN13 interval using the end of the fairly continuous presence of *Amaurolithus* spp. and the drop in its abundance (coincident with the final exit of the rare *A. primus* and *A. tricorniculatus*). They proposed this assemblage change instead of the *C. rugosus* FAD (the original definition of the NN12/NN13 boundary) because the nominate species is scattered and in very low frequency in the Western Mediterranean (Fig. 5). In the samples where we detected its presence, the frequency is less than 0.01% of the total assemblage, making it barely useful for biostratigraphic classification.

It is also noteworthy that we have detected the first *C. rugosus* close to the *G. puncticulata* entrance in the Mediterranean. The latter event has been directly calibrated in the Mediterranean to the polarity time scale (Zijderveld et al., 1986; Channell et al., this volume) as occurring at the top of the Nunivak subchron, at an estimated age of about 4.13 Ma. In oceanic areas the *C. rugosus* FAD has been placed within in the Thvera subchron (Haq and Takayama, 1984) at an age of about 4.6–4.7 Ma. It is not surprising, therefore, that the first occurrence of *C. rugosus* in the Mediterranean appears to be a migration event, strongly diachronous with respect to the open ocean.

The last occurrence of rare *A. delicatus* is recorded between the *D. asymmetricus* FCO and the *R. pseudoumbilica* LAD (Fig. 5), in the same stratigraphic position suggested by Martini (1971). However, considering its very low frequency and scattered occurrence, we also regard this event as poorly reproducible in standard analysis and not useful for biostratigraphic classification.

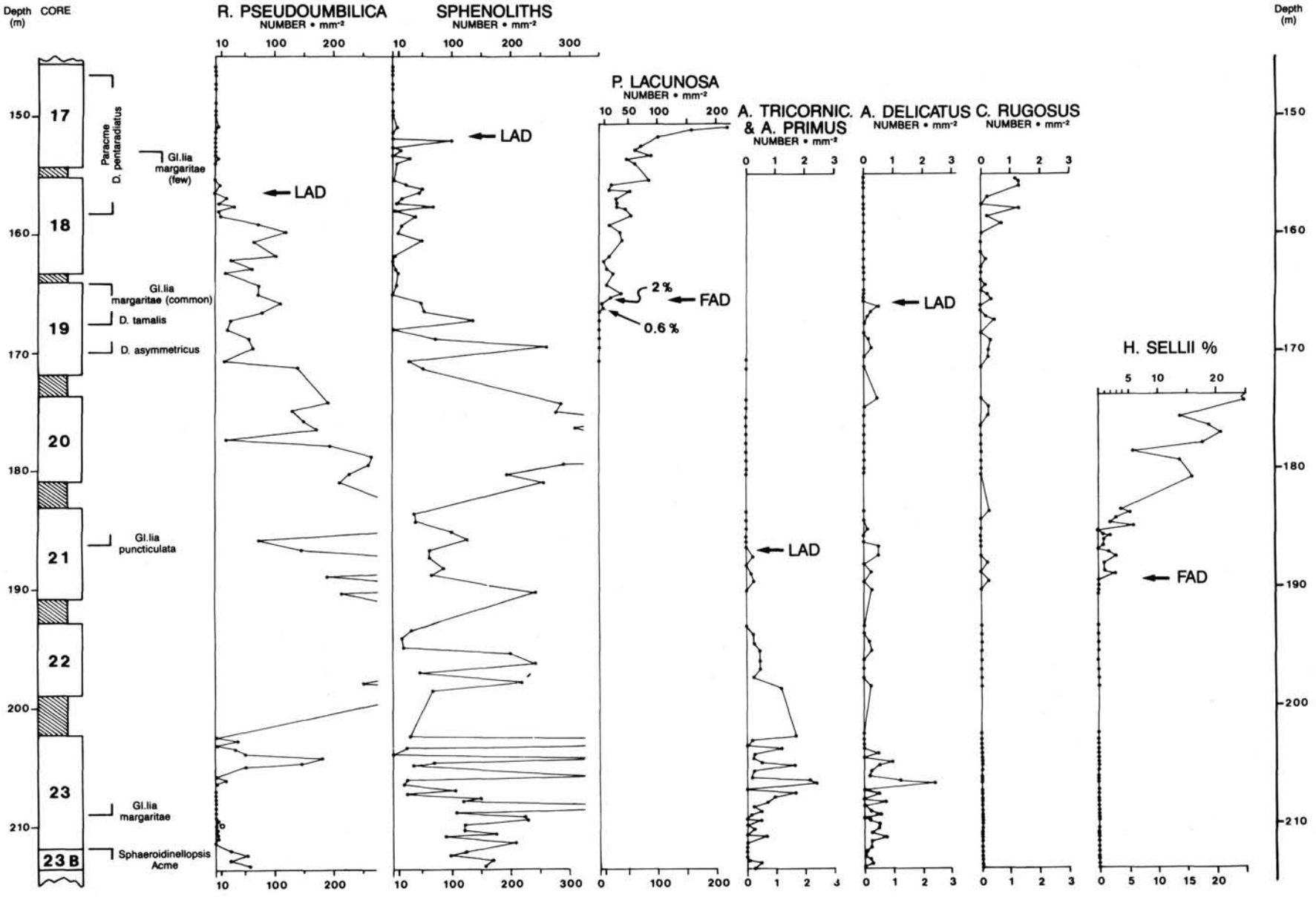

Figure 5. Abundance patterns of early Pliocene index calcareous nannofossils evaluated except for *H. sellii* by counting the number of specimens in a pre-fixed area of a slide. *H. sellii* abundance is evaluated relative to all *Helicosphaera* spp. Note the different scales used for expressing the number of specimens per mm^2. Important calcareous plankton events, described in this work and in Glaçon et al (this volume), are indicated to the right of the columnar log.

Summarizing, within the ceratholith group, the only stratigraphic event which seems consistently detectable and reproducible is the drop in abundance, continuity and species diversity of *Amaurolithus*, which occurs close to the *G. puncticulata* entrance (Fig. 5). However, recognition of this event is somewhat subjective, and we consider it a secondary event. It is be useful as supplementary evidence for locating the *H. sellii* FAD, which we use in subdividing the time interval corresponding to NN12–NN13.

Helicosphaera sellii FAD

Helicosphaera sellii has a distinct morphology (Gartner, 1977), though care must be taken with its identification because of its small size. It is reported in literature (Haq, 1973; Perch-Nielsen, 1985) as appearing in the late Miocene. However, we have not detected its presence in the lower lower Pliocene at Site 653. It is also apparently absent in onshore Italian sections of this age (i.e., the Capo Rossello section, Rio et al., 1984) and in Sites 652 and 654 (Glaçon et al, this volume).

H. sellii enters the Tyrrhenian Sea's stratigraphic record close to the appearance of *G. puncticulata* and the end of the common presence of *Amaurolithus* spp. We consider its appearance as a FAD datum (Fig. 5), but it could represent a migration event (FO) if the specimens reported from the Miocene are confirmed as belonging to the same species. We define the FAD of *H. sellii* as the increase of the species to a frequency $>1\%$ in a counting of 100 helicolithids. Since helicolithids are a common constituent of the Mediterranean Pliocene, this counting is generally easily performed in sediments of different facies, and we propose the present event as the best available in the Western Mediterranean to subdivide the long interval corresponding to NN12–NN13.

Pseudoemiliania lacunosa FAD

P. lacunosa's entrance in the stratigraphic record is not normally used in the existing calcareous nannofossil biostratigraphic schemes, except in the Raffi and Rio (1979) scheme in which it is proposed as a substitute event for the *R. pseudoumbilica* LAD. The rationale for this proposal is that the *R. pseudoumbilica* LAD is not easily recognized in Italian mainland sections, which are generally affected by strong reworking. Raffi and Rio (1979) considered the *P. lacunosa* FAD as slightly postdating the *R. pseudoumbilica* LAD. Data presented here (Fig. 5) indicate that the two species overlap for a detectable stratigraphic interval, since *P. lacunosa* appears with low frequency between the *D. asymmetricus* FCO and the *R. pseudoumbilica* LAD.

The species concept for *P. lacunosa* followed in this work is the same as discussed in Raffi and Rio (1979). The detection of the appearance of this taxon is not easy, because it is rare and it can be confused, in poorly preserved material, with small- to medium-size reticulofenestrids. It becomes abundant and more easily recognizable close to the extinction level of *R. pseudoumbilica*. We consider the *P. lacunosa* FAD as a second order event and we do not use it in our emended zonation (Fig. 2). However, we maintain that its common presence is a useful biostratigraphic indicator in terrigenous sediments in Italy, where reworking can extend the range of *R. pseudoumbilica* above its extinction level.

It is noteworthy that the *P. lacunosa* FAD at Site 653 occurs in the same biostratigraphic position and at the same interpolated age recognized in eastern North Atlantic DSDP Site 397 (see Fig. 11 and Table 3).

Reticulofenestra pseudoumbilica

The LAD of *R. pseudoumbilica* (Gartner, 1969) is used in all stratigraphic schemes proposed for the Mediterranean region (Fig. 2). Raffi and Rio (1979) used it as a secondary event because *R. pseudoumbilica* is commonly found as reworked above its true extinction level. Most probably the detection of this event is also complicated by different species concepts of *R. pseudoumbilica* among different authors. Overall size of the placolith is a critical parameter in the species definition within the reticulofenestrids. In the literature the dividing line in size between *R. pseudoumbilica* and other smaller representatives of the group generally is drawn between 5 and 6 μm (Haq and Berggren, 1978; Backman, 1980).

However, Raffi and Rio (1979) and Backman and Shackleton (1983) have noted that only the extinction of the forms larger than 7–8 μm is a distinct event at the end of the early Pliocene, while the smaller forms (5–6 μm) survived (their range and final extinction has not been established so far). Biometric results on reticulofenestrids on selected samples from Site 653 nicely document this (Fig. 6). Utilizing the biometric definition outlined above, the LAD of *R. pseudoumbilica* is an excellent event in the Mediterranean region, provided that reworking is minimal or that it can be filtered out by quantitative evaluations. As the best reproducible definition of the *R. pseudoumbilica* LAD, we propose the drop in frequency of the species below 2% of the total assemblage in a counting of 500 specimens of nannofossils.

The *R. pseudoumbilica* LAD in extra-Mediterranean sections has been calibrated as occurring in the late Gilbert Chron by Rio (1982) and Backman and Shackleton (1983). In Site 652 this event also occurs in the late Gilbert (Channell et al., this volume). At Site 653 the *R. pseudoumbilica* LAD has an interpolated age of about 3.52 Ma (Table 3) and thus seems a synchronous event over widely separated areas.

Sphenoliths

Generally, the Pliocene sphenoliths are referred to the species *S. abies* and *S. neoabies,* both of which are present in our record. However, no attempt has been made to split our specimens at specific levels, since they appear to have a synchronous extinction. Normally, it is the final extinction of the genus which is used in biostratigraphy. This makes the event unaffected by any taxonomic problems. Besides the final extinction of the genus, Ellis (1979) used the end of the acme of *S. neoabies* as a boundary event in the Eastern Mediterranean (Fig. 2).

Sphenoliths are well represented in the Mediterranean, showing abundance values which are, in some intervals, of the same order of magnitude as those recorded by Backman and Shackleton (1983) in the Tropical Indian Ocean (Core V20-163) and Equatorial Pacific Ocean (DSDP Site 504). However, the "productivity curve" of the sphenolithids shows strong variability, which seems to be cyclic in the early early Pliocene. A drop in the total abundance of this group occurs close to the *D. asymmetricus* FCO. This drop is in the same stratigraphic position as the end of the *S. neoabies* acme of Ellis (1979), and it is coincident with a major change in the calcareous nannofossil assemblage.

Our graph shows that the last sphenoliths survived the *R. pseudoumbilica* exit for a short time interval (about 0.1 m.y.), as they did in the Indian and Pacific Oceans (Backman and Shackleton, 1983). At the end of their range sphenoliths are not abundant and are actually absent in few samples. A possible operational definition for the LAD of Sphenolithus spp. is the drop of their frequency below 1% of the total assemblage in a count of 500 calcareous nannofossil specimens (Fig. 5).

Pleistocene Datum Events

Calcareous nannofossils offer a high degree of stratigraphic resolution of the Pleistocene series (Fig. 2). A significant improvement of the Martini (1971) biostratigraphic classification of the Pleistocene was introduced by Gartner (1977), who proposed 7 biozones for this time interval. In the following discus-

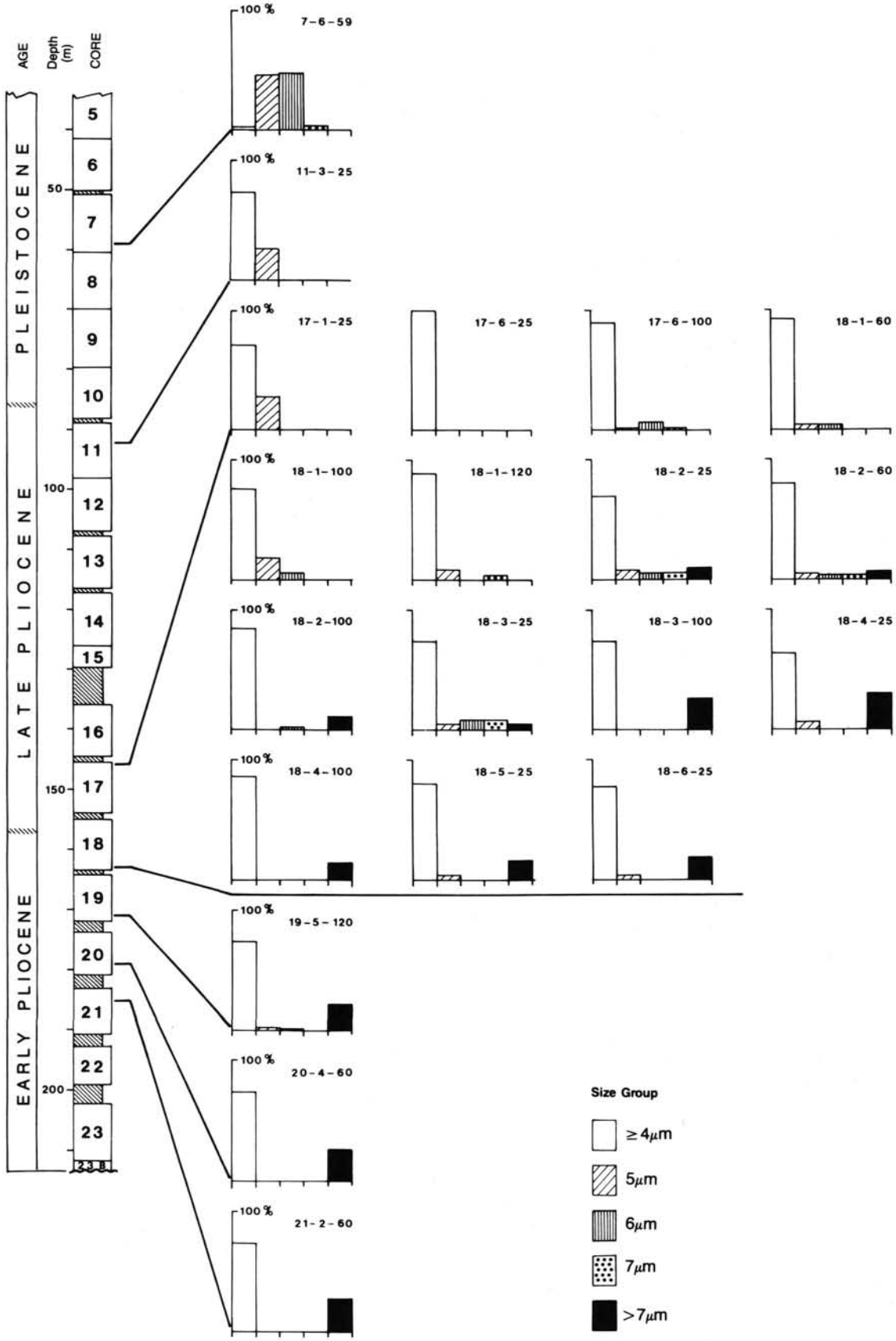

Figure 6. Reticulofenestrid placolith length distribution in selected intervals at Site 653. Fifty specimens of *Reticulofenestra* spp. ≥4 μm have been measured for each sample.

sion we will show that at least 8 datum lines, often recognized by multiple events, are easily detected in the Mediterranean allowing for the recognition of 9 biozones (Figs. 7 and 10). The stratigraphic resolution seems to be further refinable on the basis of additional local events not fully explored in this work. It should be noted that the biostratigraphic resolution provided by calcareous nannofossils for the Pleistocene is probably unmatched by any other fossil groups and it is the highest available at the present for the entire Phanerozoic time scale.

Gephyrocapsids

Gephyrocapsids were important elements in both open-ocean and neritic calcareous nannofossil assemblages during the Pleistocene, when they underwent major evolutionary changes. In spite of their abundance, wide geographic distribution and rapid evolution, gephyrocapsids have been contradictorily used by different authors for biostratigraphic classification, because their small size (2–8 μm) makes it difficult to establish their taxonomy with the optical microscope (Perch-Nielsen, 1985). It has been shown by Rio (1982), Rio et al. (in press), Williams et al. (1988) and Raffi (in preparation) that the overall size of gephyrocapsids, a feature which is easily and objectively detected with an optical microscope, does represent a plane morphometric parameter, which can be used to consistently correlate lower Pleistocene sequences from geographically distant areas.

The biometrically based definitions of the gephyrocapsid group proposed by Rio et al. (in press) has been followed here, splitting the group into four categories: (1) gephyrocapsids <3.5 μm in size labeled "small *Gephyrocapsa;*" (2) gephyrocapsids >4 μm and <5.5 μm in size, with an open central area, labeled *Gephyrocapsa oceanica* s. l.; (3) gephyrocapsids >5.5 μm in size labeled "large *Gephyrocapsa;*" (4) gephyrocapsids usually 4–6 μm in size with an open central area and a bridge nearly aligned with the short axis of the placolith, here labelled *Gephyrocapsa* sp. 3 according to Rio (1982). The latter group is comparable to *Gephyrocapsa parallela* as illustrated by Takayama and Sato (1987) and is similar to *G. oceanica* as used by authors who attach significance to the bridge orientation for the definition of gephyrocapsids at specific levels. For illustrations of each of these gephyrocapsid groups see Rio (1982).

Rio (1982), Rio et al. (in press) and Raffi et al. (in preparation) have shown that at least four events, widely recognized in the Mediterranean and in many open-ocean sequences, can be defined using the above groupings. These events are: (1) FAD of *G. oceanica* s. l. (event GO); (2) FAD of gephyrocapsids >5.5 μm (event LG); (3) LAD of gephyrocapsids >5.5 μm, which occurs synchronously with a temporary disappearance of normal sized *Gephyrocapsa* (*G. oceanica* s.l.) (event S1); (4) reentry of normal-size *Gephyrocapsa* in association with the first entrance of *Gephyrocapsa* sp. 3 (event S2). All four events listed above are easily detected at Site 653 as illustrated in Figures 7 and 8.

We have produced for *G. oceanica* s.l. a "productivity" curve (Fig. 7) and a frequency curve by counting 300 specimens of placoliths of any genus larger than 3 μm in size (Fig. 8). The two curves, compared in Figure 8, show the same position for the FAD of *G. oceanica* s.l. (GO event). It must be noted that *G. oceanica* s.l. is very rare in its lower range but later becomes a major element of the assemblage very close to the LAD of *C. macintyrei.* The coincidence of the spreading of *G. oceanica* s.l. with the LAD of *C. macintyrei* has also been noted in extra-Mediterranean areas (Raffi et al., in preparation).

For monitoring the distribution of *Gephyrocapsa* spp. >5.5 μm (large *Gephyrocapsa*) and *Gephyrocapsa* sp. 3, we have evaluated their percentage in a count of 100 *Gephyrocapsa* spp. >4 μm. *Gephyrocapsa* spp. >5.5 μm are restricted to the early early Pleistocene (Fig. 7). We define the FAD of *Gephyrocapsa* spp. >5.5 μm (LG event) as the increase of the nominate morphotype above 1% in a count of 100 gephyrocapsids >4 μm. The LAD of the same morphotype (S1 event) is defined as the drop below 1% in the same count.

Coincident with the LAD of *Gephyrocapsa* spp. >5.5 μm is the beginning of a fairly long interval of dominance of small gephyrocapsids ($<3.5\mu$m in size) which was reported by Gartner (1977) in extra-Mediterranean sections and which is characterized by the absence of *Gephrocapsa* >3.5 μm.

Gephyrocapsa sp. 3 enters the stratigraphic record at the top of this interval and its FAD (S2 event) is useful for its recognition. Apparently *Gephyrocapsa* sp. 3 is distributed only over a short interval in the Pleistocene (Fig. 7). Besides its first appearance, its local exit from the Mediterranean may prove to be a useful event to further subdivide the stratigraphic interval between the S2 event and the exit of *P. lacunosa.*

Gephyrocapsids represent a powerful biostratigraphic correlation tool in this region because they are very abundant in hemipelagic and terrigenous sediments of mainland Italy. A check of the synchroneity of these *Gephyrocapsa* events in other areas indicates that these events can be considered synchronous over wide areas (Appendix, Table 3).

Calcidiscus macintyrei

Backman and Shackleton (1983) have shown that the LAD of *C. macintyrei* is an excellent early Pleistocene event that is isochronous over widely separated geographic areas. The species may be confused with varieties of *C. leptoporus* and we believe that the different extinction levels given in the literature for *C. macintyrei* in comparison to the *D. brouweri* LAD (i.e., Backman and Shackleton, 1983 and Müller, 1984) may be due to different species concepts used by various authors.

As with gephyrocapsids and *R. pseudoumbilica,* the overall placolith size provides the criteria for objectively differentiating *C. macintyrei* from the *C. leptoporus* group. The biometry of the *C. leptoporus-C. macintyrei* group, in intervals close to its extinction (Fig. 9), shows a bimodal distribution of the length of the distal shield diameter. This indicates that, in order to be stratigraphically useful, the *C. macintyrei* species concept must be restricted to forms larger than 10 μm in size. This is in agreement with the suggestion made by Raffi and Rio (1979) and Backman and Shackleton (1983).

We have examined the *C. macintyrei* distribution patterns by determining its percentage within a 100-*Calcidiscus* count and its total abundance in a pre-fixed area. The same extinction level was determined from both approaches (Fig. 9). Accordingly, as an operational definition for the extinction of *C. macintyrei,* we propose a drop in its abundance below 1% in a 100-*Calcidiscus* count.

The age deduced at Site 653 for this event is 1.49 Ma (Appendix); Backman and Shackleton (1983) estimated it at 1.45–1.46 Ma. Considering that our age evaluation is obtained by interpolating sediment accumulation rates over a long interval, we conclude that the LAD of *C. macintyrei* is an accurate bioevent also for biochronologic evaluation.

***Helicosphaera sellii* LAD**

Backman and Shackleton (1983) demonstrated that this species has a diachronous disappearance with latitude in open-ocean sediments. Since helicolithids are generally very abundant in the Mediterranean, the exit of *H. sellii* provides a strong stratigraphic signal (Fig. 7). We have evaluated it by counting 50 helicolithids and the exit of this species is distinct in our record as it is in many other Mediterranean deep-sea (Glaçon et al., this volume) and Italian sections (Rio et al., in press). The *H. sellii* LAD can be defined as the drop of the species below 1% in a count of 50 helicolithids. This event (Fig. 7) is practically coincident with the Sl gephyrocapsid event (LAD of *Gephyrocapsa* spp. >5.5

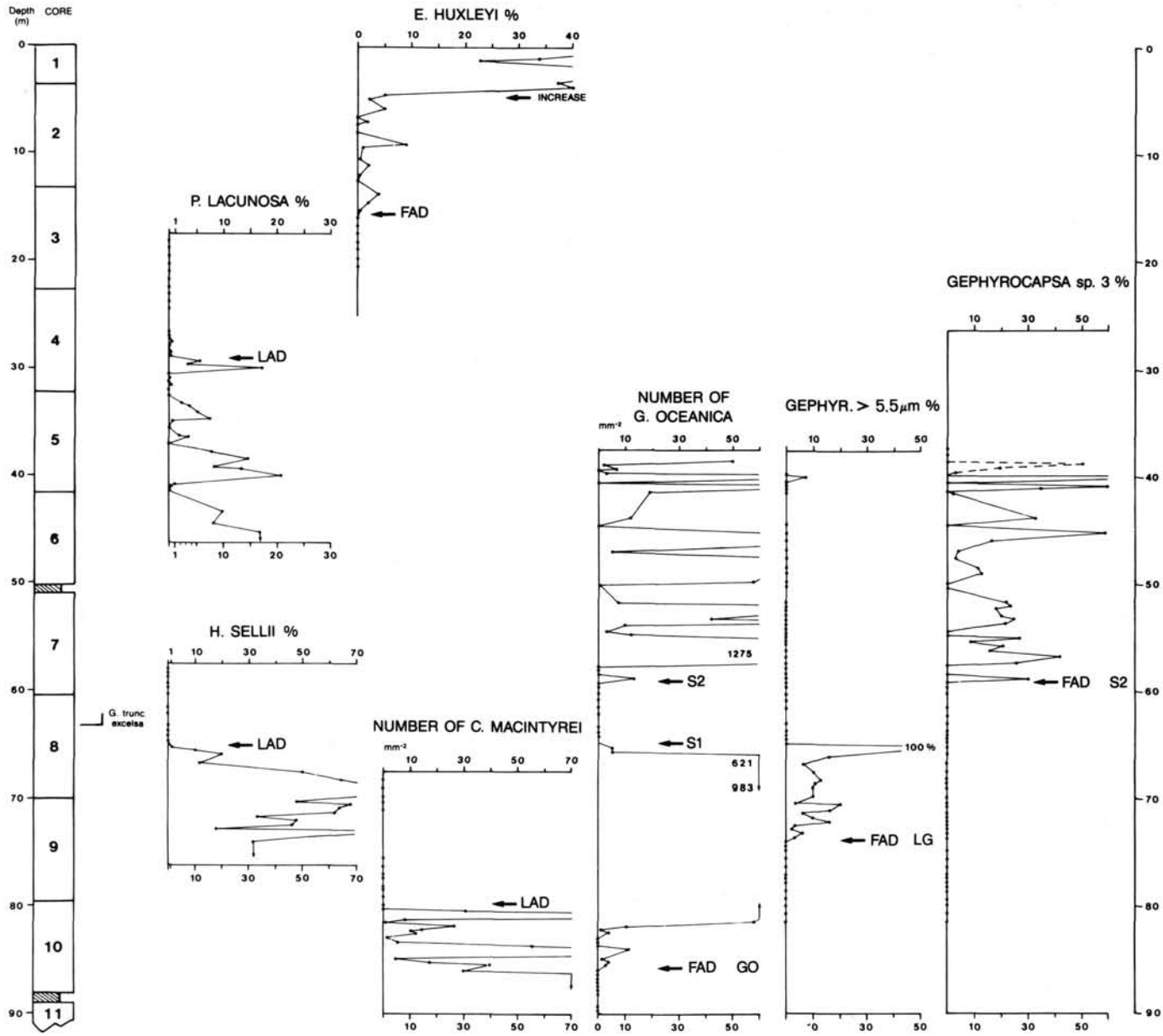

Figure 7. Abundance patterns of Pleistocene index calcareous nannofossils. See the text for a discussion of the counting methods used.

μm and the beginning of dominance of small *Gephyrocapsa* spp.).

Pseudoemiliania lacunosa LAD

At the beginning of its range *P. lacunosa* is represented by small and somewhat difficult-to-recognize specimens. In the Pleistocene it is represented by large forms, easily recognized with the light microscope in well to moderately preserved materials.

Thierstein et al. (1977) precisely defined the extinction datum of *P. lacunosa* as the midpoint of its decrease from 1% to 0% based on a count of 500 individual coccoliths. Our plot of the latest part of *P. lacunosa's* range (Fig. 7) compares well with the extinction patterns evidenced by Thierstein et al. (1977); we have, therefore, followed their definition. The event has been proven to be globally synchronous, occurring within oxygen isotope stage 12 (Thierstein et al., 1977). At Site 653 the LAD of *P. lacunosa* also occurs at the top of stage 12 (Vergnaud-Grazzini et al., this volume) and thus is synchronous with the open ocean.

Emiliania huxleyi

E. huxleyi is a small form which is more confidently recognized with an electron microscope. Three stratigraphic events have been proposed:

1. The FAD of *E. huxleyi* occurs in oxygen isotope stage 8 and is synchronous worldwide (Thierstein et al., 1977).
2. The reversal of dominance between *G. caribbeanica* and *E. huxleyi* is time-transgressive and occurs in isotope stages 5b and 5a in tropical subtropical waters and in oxygen isotope stage 4 in transitional waters (Thierstein et al., 1977).
3. The lowest level of dominant *E. huxleyi* was proposed by Gartner (1977) as definition of the base of his "*Emiliania huxleyi* Acme Zone" and, most probably, corresponds to the same event as the *G. caribbeanica/E. huxleyi* dominance reversal.

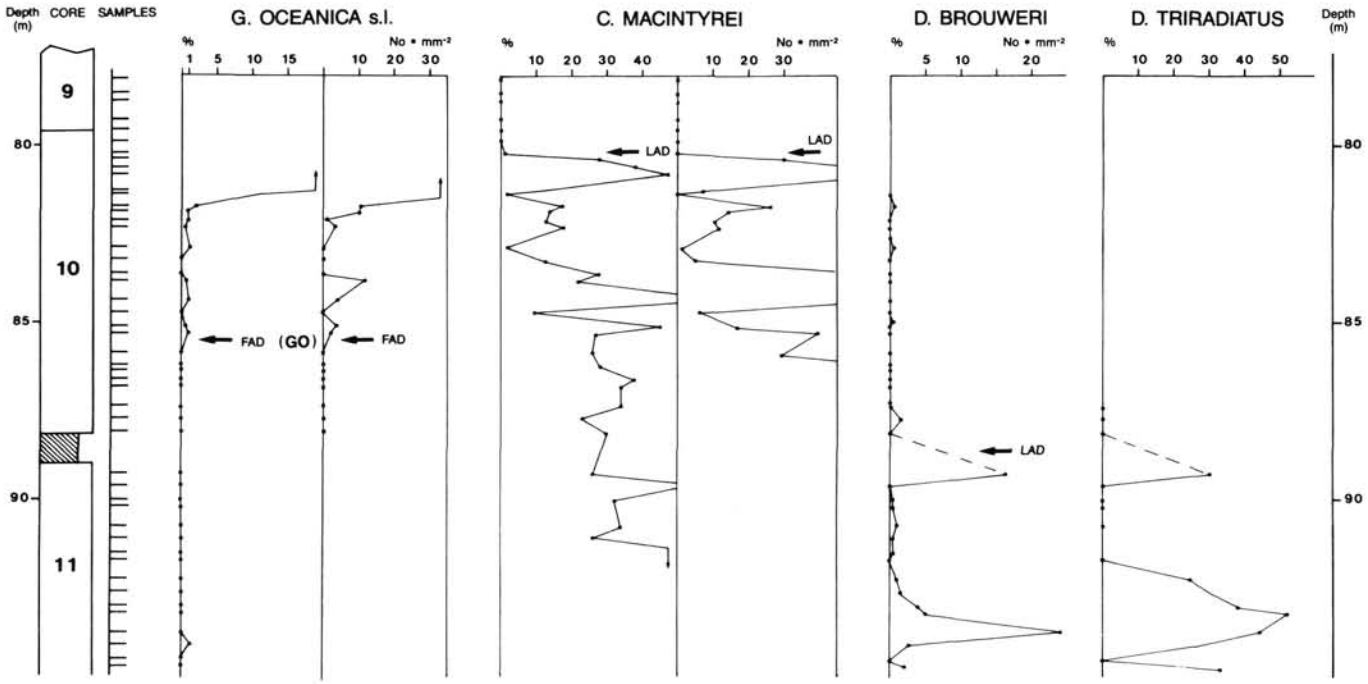

Figure 8. Calcareous nannofossil events across the Pliocene-Pleistocene boundary. Comparison of the distribution patterns of *G. oceanica* s.l. and *C. macintyrei,* close to their extinction, as provided by different counting methods is shown (see discussion in the text).

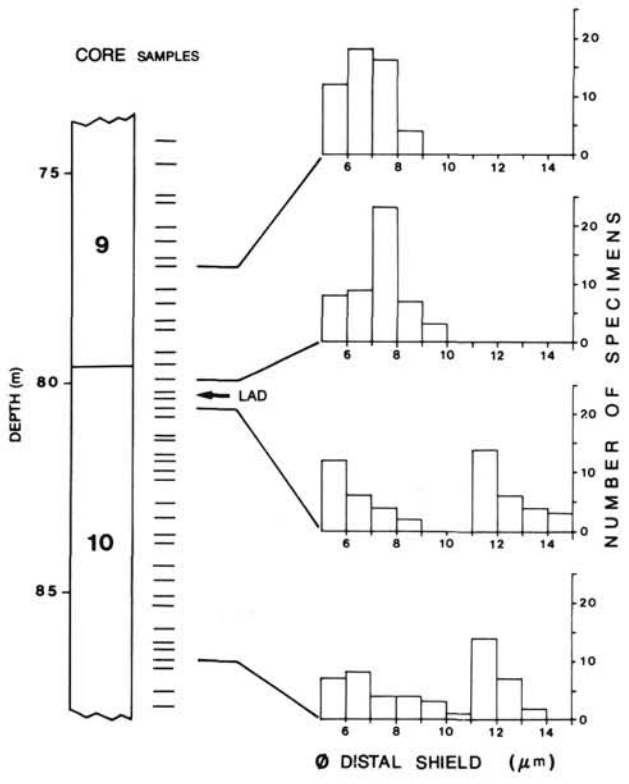

Figure 9. Placolith size distribution in the *C. macintyrei-C. leptoporus* group in the lowermost Pleistocene interval at Site 653. A total of 100 distal shields of *Calcidiscus* have been measured in each sample.

We have monitored the range of *E. huxleyi* with a scanning electron microscope (SEM), using standard techniques for preparation. Figure 7 shows plots of the relative abundance of this species based on counts of more than 300 individual coccoliths per sample (following the methodology introduced by Thierstein et al., 1977). Our results compare very well with the ranges of this taxon reported by Thierstein et al. (1977, figs. 2A and 2B), showing a lower interval of low frequency and discontinuous occurrence, followed by a sharp increase from values below 10% to values above 20%.

In agreement with Thierstein et al. (1977), we define the FAD of *E. huxleyi* as the midpoint of the slope of the initial increase of *E. huxleyi* in 300 specimens counts. The *E. huxleyi* FAD occurs at Site 653 late in oxygen isotope stage 8 as it does in extra-Mediterranean areas (Thunell et al., this volume; Vergnaud-Grazzini et al., this volume).

We have not monitored the distribution of *G. caribbeanica,* a difficult species to recognize both with the light and the electron microscope, so we are unable to locate the reversal of dominance between *G. caribbeanica* and *E. huxleyi* as defined by Thierstein et al. (1977). However, in the figures of Thierstein et al. (1977) this event is coincident with a marked increase in abundance of *E. huxleyi,* which is evident in our plots. We define the "increase of *E. huxleyi*" event as the midpoint between frequency values below and above 20%. This event is very clear in our record.

The interval of dominance of *E. huxleyi* in the latest Pleistocene and in the Holocene is easily detected with a light microscope because of the larger size attained by *E. huxleyi* late in its range. This event occurs in oxygen isotope substage 5b at Site 653 (Thunell et al., this volume) and is thus synchronous with the tropical-subtropical region of the open ocean (Thierstein et al., 1977).

BIOSTRATIGRAPHIC CLASSIFICATION

The above discussion of the calcareous nannofossil biostratigraphic events in the Mediterranean region indicates that we are

provided with a large set of reliable events suitable for biostratigraphic classification and correlation. At least 14 events can be used for zonal boundary definitions (Fig. 10) and at least 9 more events (reported as "other calcareous nannofossil events" in Fig. 10) are useful in biostratigraphic interpretation.

Many of the events do not appear in the "standard" zonations of Martini (1971) and Okada and Bukry (1980); those zonations use early Pliocene ceratolithid events barely detectable in the Western Mediterranean. As a result, some zonal boundaries of the traditional schemes cannot be recognized in the Mediterranean, and the overall biostratigraphic resolution they provide is lower than that attainable by using a local biostratigraphic scheme (Raffi and Rio, 1979). We reiterate here the need of such a local scheme and emend (Fig. 10) the zonation proposed by Raffi and Rio (1979). A comparison with previous zonations is reported in Figure 2.

Because we have already discussed at length the boundary definition events and because Raffi and Rio (1979) discussed the assemblages of the individual zones, we do not present formal definitions for each zone (self-evident in Fig. 10); instead we comment below on the main modifications introduced:

1. In the revised scheme the subzonal subdivisions are not used since all proposed biostratigraphic intervals are easy to recognize in sediments of widely different facies.
2. The zonal terminology has been updated following recent taxonomic revisions (i.e., *Calcidiscus* instead of *Cyclococcolithus, Dictyococcites productus* instead of *Cyclicargolithus doronicoides,* etc.).
3. Some zonal boundary definitions have been slightly modified (Fig. 2). The only major changes involve the boundary between the "*A. tricorniculatus* Zone" and the "*C. rugosus* Zone," which is now defined by the *H. sellii* FAD, and the definition of the "small *Gephyrocapsa* Zone" as discussed below.
4. In the latest Pleistocene-Holocene, the "*Emiliania huxleyi* Acme Zone" has been introduced and is equivalent to the zone proposed by Gartner (1977).
5. In the early Pleistocene, the "large *Gephyrocapsa* Zone" has been introduced. This interval is widely recognizable in Italian mainland sections (Rio et al., in press) and in many extra-Mediterranean regions (Takayama and Sato, 1987; Williams et al., 1988; Raffi et al., in preparation).
6. The emended zonation has been code-numbered (MNN for Mediterranean Neogene Nannoplankton) adopting the existing and widely used numbering order of Martini (1971) (Figs. 2 and 10).

A special comment is in order concerning the "small *Gephyrocapsa* Zone" of our scheme. This interval corresponds to that introduced by Gartner (1977), who defined its lower boundary by the *H. sellii* LAD and its top by the end of dominance of small *Gephyrocapsa* spp. A peculiar feature of this zone is that normal-size *Gephyrocapsa* are virtually absent. The zone has not been widely used, apparently because intervals with no normal-size gephyrocapsids occur at different stratigraphic positions within the Pleistocene.

This is also observed in our Pleistocene record (Fig. 7), in which short absence intervals of normal-size gephyrocapsids are detected. Furthermore, the LAD of *H. sellii* has been shown to be diachronous in oceanic areas (Backman and Shackleton, 1983). We adopt a different definition for this zone which should enable easier recognition: the base is defined by the S1 event, which is primarily recognized by the exit of *Gephyrocapsa* spp. >5.5 μm, and secondarily (within the Mediterranean) by the *H. sellii* LAD.

The top of the zone is primarily defined by the FAD of *Gephyrocapsa* sp. 3, and it is also recognized by the reentrance of normal-size gephyrocapsids after a fairly long absence interval. We believe that the interval defined in this way is more easily recognizable in both the Mediterranean and the open ocean, as is evident from the data presented by Rio (1982), Takayama and Sato (1987), Williams et al. (1988) and Raffi et al. (in preparation).

BIOSTRATIGRAPHIC RESOLUTION

The zonation we adopt (Figs. 2 and 10) is fairly detailed and provides a high degree of stratigraphic resolution for the Pliocene and Pleistocene marine sedimentary record of the Mediterranean. Accepting the biochronology calculated in the Appendix and reported in Figure 10, the average duration of the adopted zone is about 0.5 m.y. in the Pliocene and about 0.2 m.y. in the Pleistocene. In the Pleistocene the only fairly long interval (about 0.5 m.y.) is the *P. lacunosa* Zone. In addition, there are other calcareous nannofossil events (reported in Fig. 10) which could be used for further subdivision, once they have been shown to be widely traceable in the Mediterranean region.

Integrating the events provided by calcareous nannofossils with those provided by planktonic foraminifers, provides an extraordinary high degree of stratigraphic resolution of the Mediterranean marine Pliocene-Pleistocene record (Fig. 10). Such a framework is essential for further chronological refinements which can be obtained by using repetitive and cyclic stratigraphic signals, like rhythmic sedimentation patterns (Hilgen, 1987; Channell et al., in press) or proxy data of the climatic system (paleontological or geochemical), which are characterized by a much higher stratigraphic resolution.

CONCLUSIONS

We have presented quantitatively and semiquantitatively collected data on the stratigraphic distribution patterns of important coccoliths and discoasters in the Pliocene and Pleistocene record of Site 653. These data allow us to critically evaluate various aspects of biostratigraphic events such as mode of appearance and extinction, continuity of distribution and productivity, all of which affect the reliability of the biostratigraphic events. Data collected quantitatively are also useful in deciphering synecological and taxonomic relationships, evaluating background reworking, and establishing accurate age evaluation of the events. We have discussed the reliability of individual calcareous nannofossil events used for zonal boundaries and we have proposed operational definitions for each.

We have discussed briefly the biostratigraphic classification and resolution obtainable in the Mediterranean record using calcareous nannofossils. Specifically, we have emended the biostratigraphic scheme of Raffi and Rio (1979) by changing terminology, modifying boundary definitions, and introducing two new zones in the Pleistocene. It is evident that calcareous nannofossils provide a high degree of biochronologic resolution by means of nonrepetitive events, and as such provide an unequivocal time frame for further subdivision using physical, geochemical, or paleontological stratigraphic signals.

It is believed that through an integrated and holistic approach, the late Neogene record of the Mediterranean can be resolved with a resolution which is of the same order of magnitude as that available in oceanic sediments of late Pleistocene age.

ACKNOWLEDGMENTS

Samples for this study were provided by ODP with assistance from the National Science Foundation. We thank P. Ferrieri, E. Masini and E. Tappa for technical and computing assistance. The careful and fine reviews of K. Perch-Nielsen (Zurich) and R. Thunell (Columbia, SC) is acknowledged. K. Perch-Nielsen suggested the code numbering of Mediterranean Zonation. This work was supported by MPI and CNR grants to D. Rio.

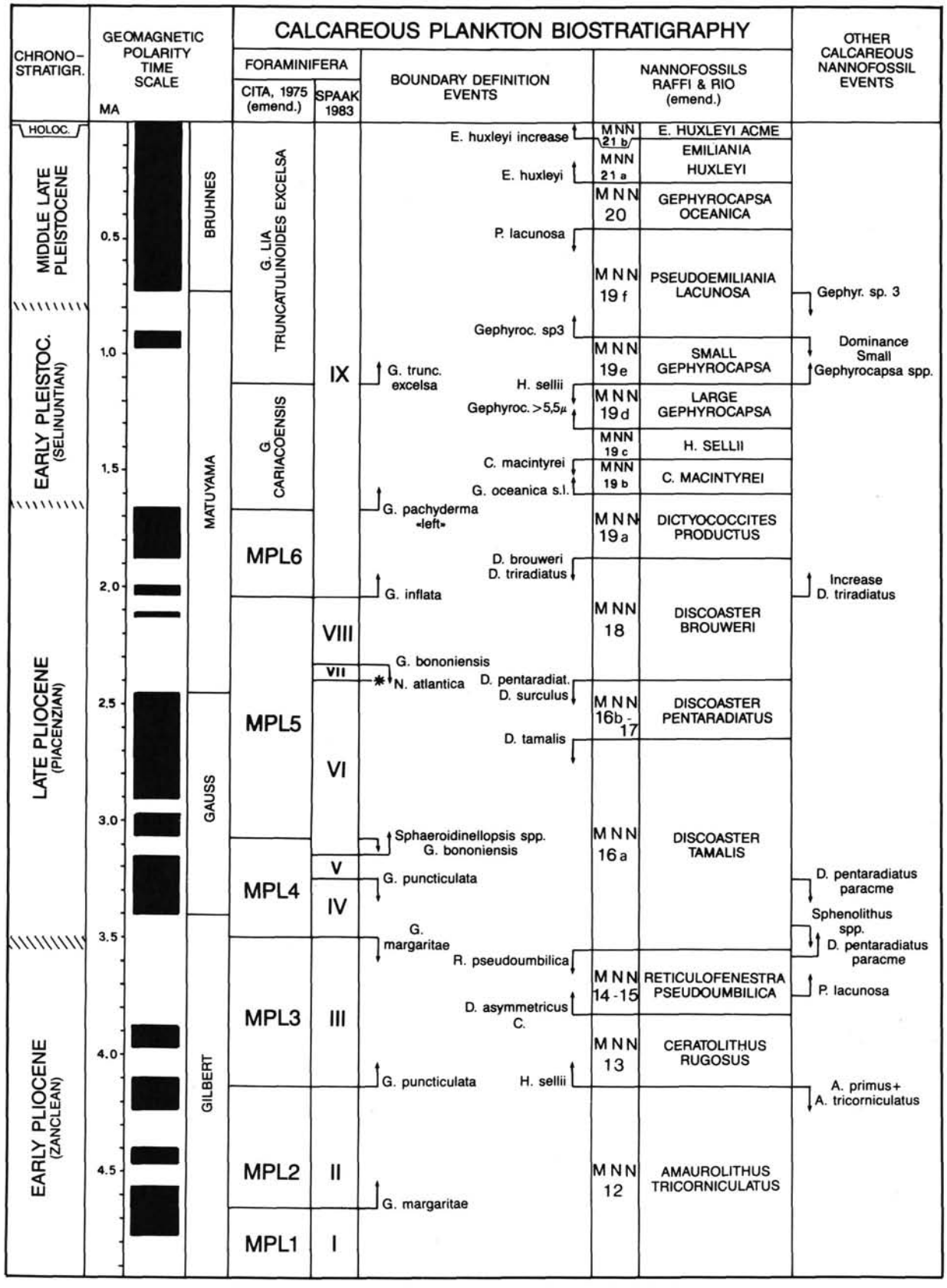

Figure 10. Calcareous plankton biostratigraphy in the Mediterranean correlated to chronostratigraphy and to the Geomagnetic Reversal Time Scale. Shown on the right are additional calcareous nannofossil events. Correlations between planktonic foraminiferal and calcareous nannofossil zones are based on the data reported in Glaçon et al. (this volume) and Rio et al. (1984). MNN = Mediterranean Neogene Nannoplankton.

REFERENCES

Backman, J., 1980. Miocene-Pliocene nannofossils and sedimentation rates in the Hatton-Rockall Basin, NE Atlantic Ocean. *Stockholm Contrib. Geol.,* 36:1–91.

_____, 1986. Accumulation patterns of Tertiary calcareous nannofossils around extinctions. *Geol. Rundschau,* 75:185–196.

Backman, J., and Pestiaux, P., 1987. Pliocene *Discoaster* abundance variations, Deep Sea Drilling Project Site 606: Biochronology and paleoenvironmental implications. *In* Ruddiman, W. F., Kidd, R. B., Thomas, E., et al., *Init. Repts. DSDP,* 94: Washington (U.S. Govt. Printing Office), 903–910.

Backman, J., Pestiaux, P., Zimmerman, H., and Hermelin, O., 1986. Paleoclimatic and paleoceanographic development in the Pliocene North Atlantic: Discoaster accumulation and coarse fraction data. *In* Summerhayes, C. P., and Shackleton, N. J. (Eds), *North Atlantic Palaeoceanography:* Geol. Soc. Spec. Publ., 21:231–242.

Backman, J. and Shackleton, N. J., 1983. Quantitative biochronology of Pliocene and early Pleistocene calcareous nannoplankton from the Atlantic, Indian and Pacific Oceans. *Mar. Micropaleontol.,* 8: 141–170.

Backman, J., Shackleton, N. J., and Tauxe, L., 1983. The Pliocene-Pleistocene at the Vrica section: Quantitative nannofossil correlation to the deep sea. *Nature,* 304:156–158.

Berggren, W. A., 1984. Neogene plankton foraminiferal biostratigraphy and biogeography: Atlantic, Mediterranean and Indo-Pacific regions. *In* Tsuchi, R. (Ed.), *Pacific Neogene Datum Planes* (IGCP Project 114): Tokyo (University Tokyo Press).

Berggren, W. A., Kent, D. V., Flynn, J. J., and Van Couvering, J. A., 1985. Cenozoic geochronology. *Geol. Soc. Am. Bull.,* 96:1407–1418.

Berggren, W. A., and Van Couvering, J. A., 1978. Biochronology. *In* Cohee, G. V., Glaessner, M. F., and Hedberg. H. (Eds.), *Contributions to the Geological Time Scale.* AAPG, Stud. Geol., 6:39–57.

Bukry, D., 1973. Low-latitude coccolith biostratigraphic zonation. *In* Edgard, N. T., Saunders, J. B., et al., *Init. Repts. DSDP,* 15: Washington (U.S. Govt. Printing Office), 685–703.

_____, 1981. Cenozoic coccoliths from the Deep Sea Drilling Project. *In* Warme, J. E., Douglas, R. C., and Winterer E. L. (Eds.), *The Deep Sea Drilling Project: A decade of Progress.* SEPM Spec. Publ., 32:335–353.

Channell, J.E.T., Rio, D., Thunell, R. C., in press. Miocene-Pliocene boundary magnetostratigraphy at Capo Spartivento (Calabria, Italy). *Geology.*

Cita, M. B., 1973. The Pliocene record in the deep-sea Mediterranean sediments: Pliocene biostratigraphy and chronostratigraphy. *In* Ryan W.B.F. et al., *Init. Repts. DSDP,* 13: Washington (U.S. Govt. Printing Office), 1343–1379.

_____, 1975. Studi sul Pliocene e gli strati di passaggio dal Miocene al Pliocene, VIII. Planktonic foraminiferal biozonation of the Mediterranean Pliocene deep sea record: a revision. *Riv. It. Paleontol. Strat.,* 81:527–544.

Crow, F. L., Davis, F. A., and Maxfield, M. W., 1960. *Statistics manual:* New York (Dover Publ., Inc.).

Dennison, J. M., and Hay, W. W., 1967. Estimating the needed sampling area for subaquatic ecologic studies. *J. Paleontol.,* 41:706–708.

Driever, B.W.M., 1981. A quantitative study of Pliocene associations of *Discoaster* from the Mediterranean. *Proc. K. Ned. Akad. Wet., Ser. B: Palaeontol., Geol., Phys., Chem.,* 84:437–455.

Ellis, C. H., 1979. Neogene Nannoplankton in Eastern Mediterranean. *Ann. Geol. Pays Hell.,* 1:391–401.

Ericson, D. B., Ewing, M., and Wollin, G., 1963. Plio-Pleistocene boundary in the deep-sea sediments. *Science,* 139:727–737.

Gartner, S., 1969. Correlation of Neogene planktonic Foraminifera and Calcareous Nannofossils zones. *Trans. Gulf Coast Assoc. Geol. Soc.,* 19:585–599.

_____, 1977. Calcareous nannofossil biostratigraphy and revised zonation of the Pleistocene. *Mar. Micropaleontol.,* 2:1–25.

Gradstein, F. M., Agterberg, F. P., Brower, J. C., and Schwarzacher W. S., 1985. *Quantitative stratigraphy* (Vol. 1): Dordrecht (D. Riedel Publ. Co.).

Haq, B. U., 1973. Evolutionary trends in the Cenozoic coccolithophore genus *Helicosphaera. Micropaleontology,* 19:32–50.

Haq, B. U., and Berggren, W. A., 1978. Late Neogene calcareous plankton biochronology of the Rio Grande Rise (South Atlantic Ocean). *J. Paleontol.,* 52:1167–1194.

Haq, B. U., and Takayama, T., 1984. Neogene calcareous nannoplankton datum planes and their calibration to magnetostratigraphy. *In* Ikebe, N., Tsuchi, R. (Eds.), *Pacific Neogene Datum Planes: Contribution to Biostratigraphy and Chronology:* (Tokyo) University of Tokyo Press, 27–32.

Hilgen, F. J., 1987. Sedimentary rhythms and high-resolution chronostratigraphic correlation in the Mediterranean Pliocene. *Newsl. Stratigr.,* 17:109–127.

Martini, E., 1971. Standard Tertiary and Quaternary calcareous nannoplankton zonation. *In* Farinacci, A. (Ed.), *Proc. II Planktonic Conf., Roma, 1970:* Roma (Tecnoscienza), 2:738–785.

Mazzei, R., Raffi, I., Rio, D., Hamilton, N., and Cita, M. B., 1979. Calibration of the late Neogene calcareous plankton datum planes with the paleomagnetic record of Site 397 and correlation with Moroccan and Mediterranean sections. *In* von Rad, U., Ryan, W.B.F. et al., *Init. Repts. DSDP,* 47, pt. 1: Washington (U.S. Govt. Printing Office), 375–389.

Müller, C., 1978. Neogene calcareous nannofossils from the Mediterranean—Leg 42A of the Deep Sea Drilling Project. *In* Hsü, K., J., Montadert, L., et al., *Init. Repts. DSDP,* 42: Washington (U.S. Printing Office), 727–751.

_____, 1984. Biostratigraphic and paleoenvironmental interpretation of the Goban Spur Region based on a study of calcareous nannoplankton. *In* Graciansky, P. C., Poag, C. W., et al., *Init. Repts. DSDP,* 80: Washington (U.S. Printing Office), 573–599.

Okada, H., and Bukry, D., 1980. Supplementary modification and introduction of code numbers to the low-latitude coccolith biostratigraphic zonation (Bukry, 1973; 1975). *Mar. Micropaleontol.,* 5:321–325.

Perch-Nielsen, K., 1985. Cenozoic calcareous nannofossils. In Bolli, H. M., Saunders, J. B., and Perch-Nielsen, K. (Eds.), *Plankton Stratigraphy:* Cambridge (Cambridge Univ. Press), 427–554.

Raffi, I., and Rio, D., 1979. Calcareous nannofossil biostratigraphy of DSDP Site 132—Leg 13 (Tyrrhenian Sea—Western Mediterranean). *Riv. It. Paleontol. Stratigr.,* 85:127–172.

Rio, D., 1982. The fossil distribution of coccolithophore genus *Gephyrocapsa* Kamptner and related Plio-Pleistocene chronostratigraphic problems. *In* Prell, W. L., Gardner, J. V., et al., *Init. Repts. DSDP,* 68: Washington (U.S. Govt. Printing Office), 325–343.

Rio, D., Backman, J., and Raffi, I., in press. Calcareous nannofossil biochronology and the Pliocene-Pleistocene boundary. *In* Van Couvering, J. (Ed.), *Final Repts. IGCP Project 41.*

Rio, D., Sprovieri, R., and Raffi, I., 1984. Calcareous plankton biostratigraphy and biochronology of the Pliocene-lower Pleistocene succession of the Capo Rossello area, Sicily. *Mar. Micropaleontol.,* 91:135–180.

Schmidt, R. R., 1973. A calcareous nannoplankton zonation for upper Miocene-Pliocene deposits from the Southern Aegean area, with a comparison to Mediterranean stratotype localities. *Proc. K. Ned. Akad. Wet., Ser. B: Palaeontol., Geol., Phys., Chem.,* 76:287–310.

Shackleton, N. J., Backman, J., Zimmerman, H., Kent, D. V., Hall, M. A., Roberts, D. G., Schnitker, D., Baldauf, J. G., Despraires, A., Homrighausen, R., Huddleston, P., Keene, J. B., Kaltemback, A. J., Krumsiek, K.A.O., Morton, A. C., Murray, J. W., and Westerberg-Smith, J., 1984. Oxygen-isotope calibration of the onset of ice-rafting and history of glaciation in the North Atlantic region. *Nature,* 3:620–623.

Shaw, A. B., 1964. *Time in stratigraphy:* New York (McGraw-Hill Book Co.).

Spaak, P., 1983. Accuracy in correlation and ecological aspects of the planktonic foraminiferal zonation of the Mediterranean Pliocene. *Utrecht Micropaleontol. Bull.,* 28:1–160.

Takayama, T., 1970. The Pliocene-Pleistocene boundary in the Lamont Core V21-98 and at Le Castella, Southern Italy, *J. Mar. Geol.,* 6: 70–77.

Takayama, T., and Sato, T., 1987. Coccolith biostratigraphy of the North Atlantic Ocean, Deep Sea Drilling Project Leg 94. *In* Ruddiman, W. F., Kidd, R. B., Thomas, E., et al., *Init. Repts. DSDP,* 94: Washington (U.S. Govt. Printing Office), 651–702.

Thierstein, H. R., Geitzenauer, K. R., and Molfino, B., 1977. Global synchroneity of late Quaternary coccolith datum levels: validation by oxygen isotopes. *Geol. Soc. Am. Bull.,* 5:400–404.

Thunell, R. C., 1979. Mediterranean Neogene planktonic foraminiferal biostratigraphy: quantitative results from DSDP Sites 125, 132 and 372. *Micropaleontology,* 25:412–437.

Williams, D. F., Thunell, R. C., Tappa, E., Rio, D., and Raffi I., 1988. Chronology of the Pleistocene oxygen isotope record: 0-1.88 million years before present. *Palaeogeogr., Palaeoclimatol., Palaeoecol.*, 64: 221–240.

Zijderveld, J.D.A., Zachariasse, J. W., Verhallen P.J.J., and Hilgen, F. J., 1986. The age of the Miocene-Pliocene boundary. *Newsl. Stratigr.*, 16:169–181.

Date of initial receipt: 8 December 1987
Date of acceptance: 17 January 1989
MS 107B-164

APPENDIX
Accumulation Rate and Calcareous Plankton Biochronology

One of the reasons for hydraulic piston coring the Site 653 sequence was to calibrate directly the Mediterranean calcareous plankton datums with the geomagnetic reversal time scale (GRTS), in order to evaluate their accuracy and synchroneity compared to extra-Mediterranean regions, and thus to establish a sound biochronological framework for the Mediterranean. Unfortunately, this goal was not accomplished because of the very weak remanent magnetization of the recovered sediments (J. Channell, pers. comm., 1987). Therefore, this direct approach to age determinations for biostratigraphic datums could not be applied.

Vergnaud-Grazzini et al. (this volume) and Thunell et al. (this volume) have produced very detailed oxygen isotope stratigraphies, which allow a sound age evaluation for three of the late Pleistocene events, the *P. lacunosa* LAD, the *E. huxleyi* FAD, and the *E. huxleyi* dominance event, and for the late Pliocene *D. surculus* LAD (see previous sections). Furthermore, a direct calibration in the Mediterranean region of the polarity time scale with several calcareous nannofossil and planktonic foraminiferal events has been achieved recently in some mainland Italian sections (Backman et al., 1983; Zijderveld et al., 1986; Channell et al., in press; Rio et al., in press) and in Site 652 (Table 3 and Channell et al., this volume).

We are provided, therefore, with some age estimates to evaluate sediment accumulation rates, to interpolate ages of events not yet calibrated, and to test their synchroneity with other regions. For this purpose, a modified "Shaw diagram" has been prepared for this site (Fig. 11). Shaw (1964) proposed this technique to compare sequences of paleontological events observed in two or more stratigraphic sections, and also for testing the normality of the event scaling, changes in the sediment accumulation rates, and stratigraphic completeness.

In the original format, a "Shaw diagram" is represented by a scatter diagram in which the sequence of events in one section is compared to the sequence of the events recorded in a section considered to be a standard reference. The best fit of the resulting scatter of homologous points is called "line of correlation." In the original formulation the technique uses as scale units the depth or thickness of the wells or outcrop sections. For the present work we use the geological time scale as the reference section, and therefore we are comparing ages instead of stratigraphic thickness. As a result, the "line of correlation" represents the accumulation rates of the considered sequence. Figure 11 was constructed using the following steps:

1. We first chose well spaced datums, using both planktonic foraminifers and calcareous nannofossils whose age calibration was considered reliable. These calibration point events are marked with a circle in Figure 11 and are reported in Table 3.
2. Thereafter we used the age estimates of intervening events (obtained in the Mediterranean region or outside) which are reported in the first and second column of Table 3. The scatter of the ages of these events are reported in Figure 11 as horizontal bars.
3. Finally, we have visually traced a "line of correlation" which fits all the ages considered (circles and horizontal bars in Fig. 11). It should be noted that this is just one of several possible "lines of correlation" as other regressions can be determined, although the resulting interpretation would not significantly affect our results.

As stated above, the "line of correlation" should be viewed as a sediment accumulation rate curve. This allows us to estimate ages of the events other than those we have used as calibration points. We have estimated the ages for the events reported in the horizontal axis of Figure 11, and these ages are summarized in Table 3. Age estimates derived in this way have been used in the considerations made discussing the single events in the previous sections.

The sediment accumulation rates in Site 653 appear quite constant for the Pliocene and early Pleistocene, becoming significantly higher in the middle and late Pleistocene. These findings are in agreement with an increase in terrigenous input during the latter interval (Mascle et al., this volume). The spacing between the *D. brouweri* LAD and the *G. oceanica* s.l. FAD is very short when compared with previous age estimates obtained in both the Mediterranean region, and a short hiatus exists between these two events that bracket the Pliocene-Pleistocene boundary. Since this hiatus seems to be missing in the DSDP Site 132 sequence, and since it occurs between two cores, it is most probably related to mechanical recovery problems.

Table 3. Biochronology of calcareous plankton events. The first two columns list events discussed in the text and abbreviation codes used to indicate the events in Figure 11. The third column shows direct age calibration of the events to Geomagnetic Reversal Time Scale (GRTS) or oxygen stable isotope stratigraphy from previous studies (as indicated). The fourth column shows age calibration to the GRTS at Site 652 (Channell et al., this volume). The fifth column summarizes ages obtained at Site 653 (see Fig. 11) by interpolation between selected calibration points (denoted CP in the table).

Code	Event	Age (Ma)	Site 652 Age (Ma)	Site 653 (Ma)
E.H.*	*E. huxleyi* increase	0.85–0.73[a]	0.85	
E.H.	*E. huxleyi* FAD	0.26[a]	0.26 CP	
P.L.T	*P. lacunosa* LAD	0.461[a]	0.46 CP	
S2	*Gephyrocapsa* sp. 3 FAD and end dominance of small *Gephyrocapsa*	0.90–0.95[b]	0.95	
S1	Base of dominance of small *Gephyrocapsa* and *H. sellii* LAD	1.10–1.15[b]	1.10	CP
L.G.	*Gephyrocapsa* spp. >5.5 μm FAD	1.29–1.34[b]	1.32	
C.M.	*C. macintyrei* LAD	1.45–1.46[c]		1.49
G.O.	*G. oceanica* s.l. FAD	1.55–1.61[b]	1.62	CP
D.B.	*D. brouweri* LAD	1.89[c]	1.80	1.83–1.87
G.I.	*Globorotalia inflata* FO			2.10
D.B.3	*D. triradiatus* increase (>40%)	2.07[c]		2.10
G.B.T	*G. bononiensis* LO			2.35
D.D.	*Discoaster* decrease	2.4	2.41–2.42	2.41 CP
D.T.	*D. tamalis* LAD	2.65–2.67[c]	2.54–2.56	2.60
S.S.	*S. seminulina* LAD	3.05–3.10[d]	3.03–3.04	3.02
G.B.B	*G. bononiensis* FO	3.15–3.16	3.07	
P2	*D. pentaradiatus* end paracme			3.27
G.P.T	*G. puncticulata* LO		3.18–3.27	3.27
SPH.	*Sphenolithus* spp. LAD	3.43–3.47[c]	3.35–3.36	3.41
R.P.	*R. pseudoumbilica LAD*	3.50–3.56[c]	3.50–3.60	3.52
P1	*D. pentaradiatus* beginning paracme			3.55
P.L.B	*P. lacunosa* FAD	3.49–3.72[e]		3.74
A.D.	*A. delicatus* LAD	3.65–3.85[e]		3.75
D.A.	*D. asymmetricus* FCO	3.90[e]	3.83	3.84 CP
G.P.B	*G. puncticulata* FO	4.13[f]	4.09–4.11	4.13 CP
A.M.	*Amaurolithus* spp. LCO			4.13
H.S.B	*H. sellii* FO			4.16
G.M.B	*G. margaritae* FO	4.65–4.66[f]	4.70–4.71	4.66 CP

Note: Footnotes refer to references for age calibrations shown in the third column.
[a] Thierstein et al. (1977).
[b] Rio et al. (in press).
[c] Backman and Shackleton (1983).
[d] Rio et al. (1984).
[e] Mazzei et al. (1979).
[f] Zijderveld et al. (1986).

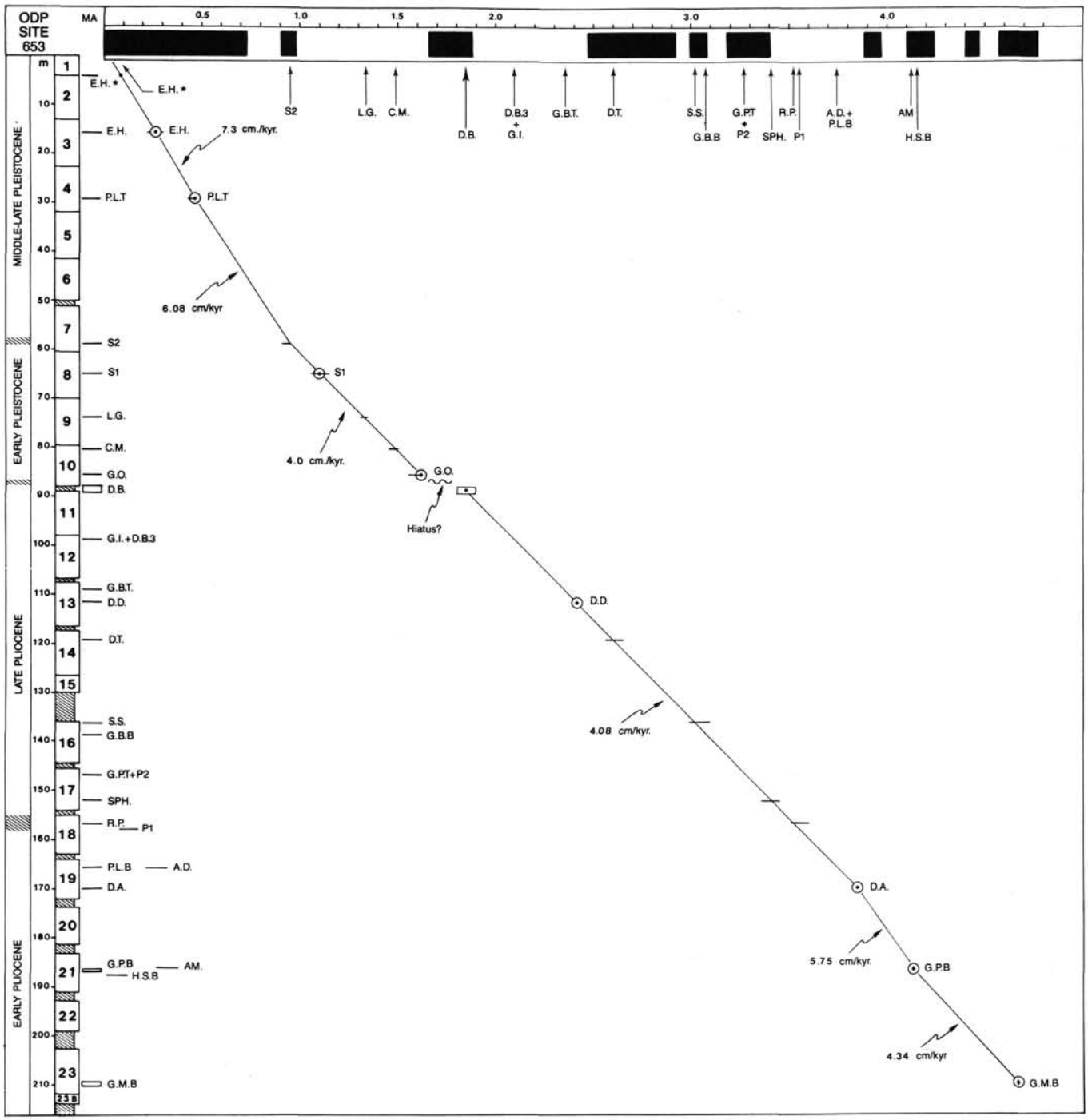

Figure 11. Sediment accumulation curve at Site 653. See the Appendix and Table 3 for explanations and abbreviations of events. Foraminiferal datums are derived from Glaçon et al. (this volume).